Anna Jonhed

Properties of modified starches and their use in the surface treatment of paper

Anna Jonhed

Properties of modified starches and their use in the surface treatment of paper

ABSTRACT

The papermaking industry uses a large amount of starch each year, both as a wet-end additive and as a rheological modifier in surface sizing and coating colors. It is important to be able to reduce the amount of chemicals used in the papermaking and surface treatment process, to reduce costs and to make the process even more efficient. Interest in new high-performance starches is great. By using these new types of starches, improved recycling of barrier products may be obtained as well as a reduction in the use of synthetic sizing agents.

The objectives of this work were to understand the behavior of temperature-responsive hydrophobically modified starches, where the solubility in water simply can be adjusted by temperature or by polymer charge, to improve the barrier properties of papers surface sized by starch-containing solutions, and to investigate the potential for industrial use of these temperature-responsive starches.

It was demonstrated that the temperature-responsive starches phase separate upon cooling and, depending on the charge density of the starch, a particulate precipitation or a gel-like structure was obtained. The starch with zero net charge showed a larger increase in turbidity than the starch with a cationic net charge, indicating that particulate precipitation is favored by a zero net charge and that the formation of a gel network is favored by charged starch molecules. Further, the starches formed inclusion complexes with surfactants, giving stabilization to the starches in the presence of surfactants. The net charge density of the starch and the charge of the surfactant determined whether or not an inclusion complex would form between them. Important mechanisms for the stability of the starch seemed to be formation of mixed micellar-like structures between the hydrophobic chain of the starch and the surfactant along the starch backbone in addition to formation of inclusion complexes between the starch and the surfactant.

The hydrophobically modified starches showed higher hydrophobic surface character when applied to the paper surface above the critical phase separation temperature than with application at room temperature. Free films of the temperature-responsive starches showed good barrier against oxygen, but no barrier against water vapor. The mechanical properties of the films decreased with addition of glycerol.

Papers included in this thesis

The following papers are included in this thesis and are referred to by their Roman numerals in the text:

I   Jonhed, A., Järnström, L.,
    Phase and gelation behavior of 2-hydroxy-3-(N,N-dimethyl-N-dodecylammonium)propyloxy starches
    Starch, **2003**, *55*, 569-575

II Jonhed, A., Järnström, L.,
    The interaction between surfactants and 2-hydroxy-3-(N,N-dimethyl-N-dodecylammonium)propyloxy starches
    Accepted for publication in Starch

III Jonhed, A., Järnström, L.,
    Influence of polymer charge, temperature and surfactants on surface sizing of liner and greaseproof with hydrophobically modified starch
    Submitted to Tappi Journal

IV Jonhed, A., Andersson, C., Järnström, L.,
    Effects of film forming and hydrophobic properties of starches on surface sized packaging paper
    Submitted to Packaging Technology and Science

Reprints of the articles have been made with permission from the publishers.

Related presentations and reports by the same author:

Jonhed, A., Järnström, L.,
   Interaction between surfactants and 2-hydroxy-3-(N,N-dimehtyl-N-dodecylammonium)propyloxy starches
   Presented at the 229th ACS National Meeting, San Diego, CA, USA,
   March 13-17, 2005

Jonhed, A., Järnström, L.,
   Phase separation behavior of chemically modified starches
   Presented at the 225th ACS National Meeting, New Orleans, LA, USA,
   March 23-27, 2003

Jonhed, A., Mesic, B., Hjärthag, C. and Järnström, L.,
   Starch modifications for surface properties
   Presented at Pira 3rd Int. Sizing Conf.: Scientific and Technical Advances in
   Internal and Surface Sizing, Prague, December 2001, Paper 18

Andersson, C., Jonhed, A., Järnström, L.,
   Characterization of modified starches for film preparation
   Manuscript

TABLE OF CONTENT

1   INTRODUCTION

Starch is the reserve carbohydrate in the plant kingdom, where it is generally deposited in the form of well-organized granules that are insoluble in cold water (Wurzburg 1986). Starch has been used in various industrial applications for many years. The paper industry uses starch extensively for various applications, the food industry uses starches for viscosity control while the pharmaceutical industry uses starches as fillers and carrier materials.

1.1   Starch in the surface treatment of paper and board

In papermaking, starch is the third largest component by weight, surpassed only by cellulose fiber and mineral pigments (Maurer 2001). This makes the paper industry one of the most important customers for the starch industry. The main application areas for starch within the papermaking process are (Maurer 2001):

- Furnish preparation prior to web formation – starch is used as a flocculating agent and retention aid, and to improve internal sheet strength.
- Surface sizing – starch is used as an adhesive to bond vessel segments and loose fibers at the sheet surface, to enhance paper strength and stiffness, to give dimensional stability and improve offset printability.
- Coating – starch is used as a binder for pigments.
- Effluent treatment – starch is used as a cationic polymer in waste treatment to control the discharge of cellulose fibers, pigments and other components of the papermaking furnish.
- Conversion of paperboard to packaging grades – starch is used as an adhesive in the manufacture of multi-ply board and for corrugating and laminating operations.

Starch is added to paper to increase its strength both in internal and surface sizing (Muller, 2000). Only about 60% of the unmodified starch is retained on cellulose

fibers in one-pass retention (Cushing et al. 1959). A significantly better retention, almost 100%, is achieved with cationic starch (Moeller, 1966). The binding power of cationic starch is greater than that of a native starch because the ionic interactions between the starch, fibers and fillers are stronger than simple hydrogen bonds. In addition, the greater stability of the molecules of the modified starch and their inherently better rheology make them useful at higher molecular weights without runnability problems. These starches also have a greater binding power compared to unmodified starches (Glittenberg and Becker 1998).

1.2   Surface treatment - sizing and coating

Most grades of paper and board need to be resistant to wetting and penetration by liquids. The properties of the final paper surface can be modified in several different ways, the most important being surface sizing, coating and calendering (Neimo 2000).

1.2.1   Surface Sizing

Surface sizing is a process whereby chemical additives are applied to provide the paper with resistance to wetting and penetration of liquids, i.e. make it more water-repellent (Neimo 2000) and to bind the particles in the surface and increase the surface strength. Internal sizing is a process where chemicals are added to the paper stock and retained on the fibers in the wet end. Surface sizing, which is studied in this thesis, is the application of a size to the web surface at the dry end of the process. Starch is the most frequently used binder in surface sizing. Besides raising the surface strength, starch addition also lowers water sensitivity, reduces dimensional changes, imparts stiffness, and raises air-leak density of the sheet (Maurer 2001) and it also improves the tensile strength and internal bonding of the paper. Cationic starch has been used extensively for surface sizing since it gives better binding power than native starch, because ionic interactions are stronger than simple hydrogen bonds (Glittenberg and Becker 1998).

_____

1.2.2 Coating

Paper coating is a process in which a coating color is applied to the paper surface to alter the surface properties of the final paper product. If the paper is coated, the voids on the paper surface are diminished and the final paper surface becomes smooth with controlled porosity. Printing ink absorbs better to a smooth surface, i.e. the ink penetration is more even compared to un-coated surfaces and the risk of mottling decreases. The coating also influences the brightness, opacity and the gloss of the paper (Fellers and Norman 1996). The brightness can increase depending on the particle size of the pigments in the coating color, while the opacity and the gloss increases when coating the paper. Starch is a common binder in coating colors. It is used as a sole binder or in combination with various synthetic binders such as polymeric emulsions or co-polymers of e.g. styrene butadiene. The use of starch as a coating binder is limited by its sensitivity to water and high surface energy. Starch provides benefits by raising the coated paper stiffness, but it can also lead to cracking at the fold after web offset printing. Coating formulae provide dispersive, thickening, lubrication, leveling, and preservative functions (Maurer 2001). Fast immobilization of cationic coating colors on anionic paper surfaces improves the fiber coverage and the printability (Lee et al. 2002).

1.3 Starch in surface treatment

A paper surface sized by the application of starch can resist penetration of water over a relatively long period of time despite its hydrophilic character. However, the application of a modified starch improves the resistance to water.
Starch ethers and some starch esters are most widely used as coating binders (Maurer 2001). Oxidized starches, starch ethers, and starch esters are resistant to retrogradation and their dispersions can be held at a lower temperature than is required for the products of chemical or thermal/chemical conversion. Hydrophobized starches present another new product class for coating application but they have so far found only limited application (Maurer, 2001).

Interest in new "special" grades of starch in paper coating and paper surface sizing is constantly increasing. Examples can be found in new concepts for ink-jet papers,

coatings with greater fiber coverage, etc. Several of the new starch grades are hydrophobically modified. Hydrophobically modified starches can be synthesized as anionic (Wurzburg 1986), cationic (Glittenberg and Becker 1998) or non-ionic (Wesslén 1998) derivatives. Several of the hydrophobic starches, such as the benzyl starches, suffer from poor stability and cannot be used commercially as paper additives. However, two of the most promising and recently most investigated derivatives are the substituted succinate derivatives and the derivatives of epoxypropyldimethylalkyl-ammonium chloride. The succinate derivatives have one negative charge attached to each pendant hydrophobe and the hydrophobic quaternary ammonium derivatives have one permanent positive charge attached to each pendant hydrophobic group. Both the succinate and the quaternary ammonium reagents form products that are used in the paper field. This thesis focuses on starch modified by a quaternary ammonium reagent.

1.4 Objectives of Thesis

The aim of this study was to investigate the behavior of hydrophobically modified (HM) potato starch in solution and further, the final surface properties of a substrate sized with HM starch compared to starches conventionally used in the paper industry today. The final surface properties when using the HM starch in surface sizing applications are of great importance.

The starch behavior in solution was studied on a molecular level by rheological and spectroscopic methods (Paper I). Surfactants were used to investigate the interaction between HM starch and hydrophobes and to gain understanding about the phase separation mechanism. The interaction of the HM starches in solution with surfactants was investigated by differential scanning calorimetry and turbidity measurements (Paper II). This is of interest since many coating colors contain latices that are stabilized by surfactants. In Paper III, the surface sizing effect of the HM starches was investigated by bench coating trials and several surface analyses. Finally, free films of the HM starches were studied to gain information about their barrier and mechanical properties together (Paper IV). Further, the influence of glycerol in the starch films and surface sizing was investigated.

2 POLYMERS IN AQUEOUS SOLUTION

2.1 Polymer association in aqueous solution

When a polymer is submerged in water, its conformation depends on the water-polymer interaction (Painter and Coleman 1997). Polymer molecules can adopt three configurations: a compact sphere, a random coil, and a stiff rod. However, the polymers usually adopt a configuration intermediate between these configurations. If the polymer-solvent interaction is unfavorable, the polymer will form a sphere to avoid contact with the solvent. If the polymer is flexible and the polymer-solvent interaction is favorable, a random coil will be formed. If the polymer is stiff like a double helix (like DNA) or highly charged, the rod configuration will occur.

Polymer solutions can be divided into three concentration regimes; dilute, semi-dilute and concentrated. In a dilute solution, the distance between individual polymers is considerably longer than the radius of a polymer coil and the polymer molecules can adopt an unconstrained configuration as they are not in contact. In the semi-dilute region, the molecules start to interact with each other. A semi-dilute solution develops when the polymer concentration exceeds c^*, the overlapping concentration, where the average distance between the polymer coils is approximately twice the individual polymer coil radius. The viscosity increases more rapidly with increasing polymer concentration in this regime than in the dilute solution. Most polymer solutions are in the semi-dilute regime with a c^* of the order of 0.1-5 wt%. c^* depends on the molecular weight of the polymer. In a concentrated solution, polymer molecules are highly entangled and have properties close to a polymer melt (Evans and Wennerström 1999). Such high concentrations are not considered in this thesis.

2.2   Solubility of polymers in aqueous solution

The requirements for two liquids to be miscible is that the change in Gibb's free energy, ΔG, is $\Delta G < 0$. The Bragg-Williams (BW) theory is the basis for the Flory-Huggins (FL) theory of polymer solutions. The BW model is based on a lattice model where each site can accommodate one molecule irrespective of type and size, the mixture is random (*Figure 2.1*).

x	x	x	x	x
x	x	x	x	x
x	x	x	x	x
x	x	x	x	x
x	x	x	x	x

$+$

o	o	o	o	o
o	o	o	o	o
o	o	o	o	o
o	o	o	o	o
o	o	o	o	o

$\rightarrow$

x	o	x	x	o	x	o	o	x	o
o	o	x	o	o	x	o	o	x	x
x	o	x	o	o	x	o	o	o	o
o	x	o	x	x	o	x	x	x	x
x	o	x	o	x	x	o	o	o	o
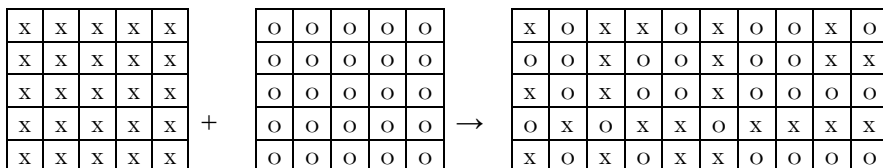
Figure 2.1. *Lattice model for the random mixing of two liquids A and B, where x=A and o=B.*

This means that the number of neighbors is always constant, assuming that all lattice positions are occupied and that the volume does not change upon mixing. The interaction is limited to the neighbors. The mixing energy is therefore non-zero, $\Delta H \neq 0$, while the mixing entropy is ideal, $\Delta S = \Delta S_{ideal}$ (Jönsson et al. 1999).

The Flory-Huggins model was proposed independently by Flory (Flory 1942; Flory 1953) and Huggins (Huggins 1942) and is valid for polymers in the semi-dilute regime. One polymer segment or one solvent molecule can be in each cell in the lattice (*Figure 2.2*). The procedure in the Flory-Huggins model is to first place the polymer chains in the lattices and then fill up the empty cells with solvent molecules.
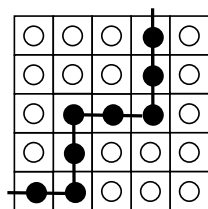
Figure 2.2 *Lattice model for the Flory-Huggins model. The filled circles represent polymer segments connected to each other and the open circles solvent molecules.*

The entropy change in mixing a polymer and a solvent is smaller than in the BW model, since the monomers in the polymers are not fully capable of exploiting the

volume increase upon mixing – the connectivity of the polymer prevents this. The entropy of mixing can be derived as

$$\Delta S_{mix} = k_B \left[(\phi / N) \ln \phi + (1 - \phi) \ln(1 - \phi) \right] \qquad [2.1]$$

where k_B is the Boltzmann constant, ϕ is the volume fraction of polymer in solution and N is the number of segments of polymer. The enthalpy of mixing can be derived as

$$\Delta H_{mix} = k_B T \chi \phi (1 - \phi) \qquad [2.2]$$

where T is the absolute temperature and χ is the dimensionless interaction parameter introduced by Flory. The interaction between segment-solvent can be described by the interaction parameter, χ. The χ-parameter is defined as the energy change associated with the transfer of a solvent molecule to pure polymer, normalized by dividing by kT. If the solvent and the polymer have the same polarity, $\chi = 0$ and in a good solvent the volume exclusion leads to swelling of the polymer (strong chain expansion) (Fleer et al. 1993). The total free energy of mixing can be written as

$$\Delta G = \Delta H - T \Delta S = k_B T \left(\frac{\phi}{N} \ln \phi + (1 - \phi) \ln(1 - \phi) + \chi \phi (1 - \phi) \right) \qquad [2.3]$$

If the value of χ is specified, the free energy of mixing for the polymer solution can be determined. The phase behavior at a given temperature can then be derived using equation 2.3.

If the polymer segments and the solvent molecules prefer to mix, then the interaction parameter is positive. When $\chi > 0.5$, a strong attraction is indicated between like components and the conditions for dissolving the polymer in the solvent are considered bad, whereas $\chi < 0.5$ indicates good solvent conditions. The transition point between the two solvent conditions at $\chi = 0.5$ is called the θ–point.

In the original Flory theory, χ was defined as a contact enthalpy divided by kT, where k is the Boltzmann constant (Fleer et al. 1993). This meant that at high temperatures all solvents are good solvents. This has not been found to be true experimentally. If volume fraction of polymer is plotted as a function of temperature, two curves are obtained; one convex at high temperatures and one

concave at low temperatures. These temperatures at the minimum and maximum are the lower and upper critical solution temperature (LCST and UCST), respectively. *Figure 2.3* shows the temperature dependence of the interaction parameter (χ). It has been stated that not only differences in contact enthalpy, but also differences in free volume between polymer and solvent contribute to the χ - parameter, which means that $\chi = \chi_c + \chi_f$, where χ_f is the contribution of the free volume. Both χ_c and χ_f are dependent of the reduced molar volume and χ_c decreases with temperature, while χ_f increases.
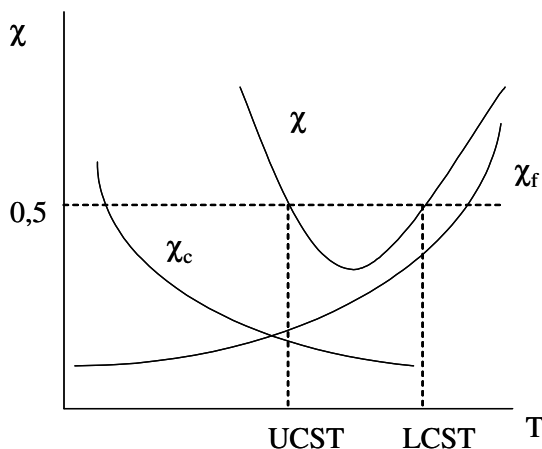
Figure 2.3. *Dependence of the Flory-Huggins χ-parameter and its contributions χ_f and χ_c on the temperature where UCST and LCST are marked as well.*

The intersection of the line of $\chi = 0.5$ with the curve for χ gives UCST and LCST as indicated in Figure 2.3. The stable region of the phase diagram is found between these two temperatures, where χ passes through a minimum.

2.3 Phase separation

For a given solvency, a solution will separate into a dilute solution and a concentrated solution. Polymer solutions can phase separate in two ways; by segregation or by associate phase separation. If there is a strong attraction between

_____

the two polymers, an associative phase separation occurs with one phase being concentrated in the polymer and the other phase being a dilute solution. A high molecular weight of the polymer induces a high degree of phase separation (Jönsson et al. 1999).

The starch solution separates and becomes cloudy, and the critical temperature is also referred to the clouding point of the polymer. The temperature-responsive HM starches phase separate and, depending on the net charge of the starch either a particulate precipitation together with a clear solution is obtained, or a gel-like structure is formed, when the starch solution is cooled (Paper I; Fleer et al. 1993). A zero net charge promoted particulate precipitation while a cationic net charge favored gel network formation for the HM starches.

For binary polymer solution consisting of one polymer dissolved in a solvent, the phase behavior is commonly plotted as the temperature versus the concentration in a phase diagram. In the Flory-Huggins theory, the critical interaction parameter (χ_c) and the critical concentration (ϕ_c) for phase separation in a binary polymer solution can be expressed as

$$\chi_c = \frac{(1+\sqrt{N})^2}{2N} \qquad\qquad\qquad [2.4]$$

$$\phi_c = \frac{1}{1+\sqrt{N}} \qquad\qquad\qquad [2.5]$$

For polymers of infinite length, $\chi_c = 0.5$ and for a monomer $\chi_c = 2$. This indicates that the monomer is more soluble than the polymer and that the polymer can more easily phase separate (Jönsson et al., 1999).

2.4 Hydrophobically modified polymer association in aqueous solution

Modification of water-soluble polymers by grafting a low amount (about 1% of the monomers reacted) of hydrophobic groups, like alkyl chains, leads to amphiphilic polymers which have a tendency to self-associate by hydrophobic interaction (Jönsson et al. 1999). The phase behavior of hydrophobically modified (HM) non-

ionic polymers has been studied for a long time. Extensive studies have been directed towards understanding the associative behavior of HM cellulose ethers (Landoll 1982). HM polymers, like the quaternary amine-modified starches used in this thesis, are also called associative thickeners. They are able to modify the rheological properties of a solution by interacting with other compounds, e.g. surfactants and other polymers. The interaction between HM polymers and surfactants will be discussed in Section 4.2.

Water-soluble HM polymers often have properties significantly different from those of their corresponding unmodified parent polymers. Association of these polymers is driven by the hydrophobic interaction between grafted tails on the same polymer or tails on neighboring polymers; it can be either intra- or inter-molecular (*Figure 2.4*). In dilute solutions, the associations are mainly intra-molecular resulting in a polymer coil more compact than the corresponding unmodified polymer (Tanaka et al. 1990). These hydrophobic polymers start to associate at concentrations below the overlap concentration of the corresponding unmodified polymers due to the hydrophobes. As the polymer concentration increases, the HM polymers start to inter-associate resulting in a three-dimensional network which leads to an increase in viscosity (Glass 1989; Winnik and Yekta 1997). This viscosity-increasing effect is a very important property of the HM polymers. Many HM polymers form less defined aggregates in which the hydrophobes associate into micelle-like structures.

a   b
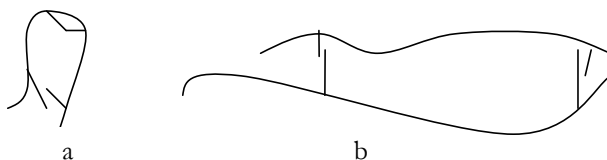
Figure 2.4. *Structures formed in a solution with HM polymers. Intra-association (a) and inter-association (b).*

3   STARCH

Starch is a naturally occurring high-molecular weight polymer of α-D-glucose and it is not only the main energy reservoir of higher plants but also a major source of energy in human and animal diets. The reserve starch of higher plants is formed in the amyloplasts. One amyloplast may contain one starch granule (e.g. potato and maize) or it may contain several granules (e.g. rice).

Starch consists of two main fractions: amylose (section 3.1) and amylopectin (section 3.2). Amylose is almost linear while amylopectin is a highly branched polymer. Amylose and amylopectin possess different properties and are therefore best suited for different applications (Zobel 1988).
The ratio of the amylose to amylopectin varies together with the chain length distribution, granular size, and lipid content in starches from different sources. Regular potato starch contains about 20% amylose and 80% amylopectin (Wurzburg 1986).

3.1   Amylose

Amylose is an almost linear, water-soluble polysaccharide with α-D-1,4-anhydroglucose linkages. The molecular weight of amylose is 10^5-10^6 Da, *Figure 3.1* (Whistler et al. 1984; Buléon et al. 1998) for most starch sources. The molecular size depends on the source and it may contain anywhere from about 200 to 2000 anhydroglucose units. Because of its linearity, mobility and hydroxyl groups, the amylose polymers have a tendency to orient themselves in a parallel fashion where hydrogen bonds can be formed between adjacent polymers. This phenomenon of intermolecular association is commonly called retrogradation (Wurzburg 1986) and as a result the amylose gels become opaque (see section 3.4).
Although it is said that amylose is linear, it is well established that there is some branching on the molecule. These few branches do not influence the

_____

hydrodynamic behavior of amylose (Buléon et al. 1998). The configuration of amylose is still open to debate (Whistler et al. 1984) but it is said that in water, amylose exists as a random coil, whereas in a good solvent (e.g. dimethylsulphoxide) it exists as an extended coil. In the presence of a complexing agent (e.g. I$_2$ or lipids) amylose exists as a helix (Banks and Greenwood 1975).
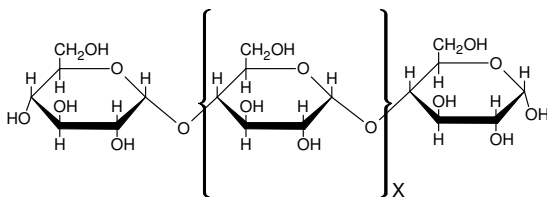
Figure 3.1. *The chemical structure of amylose.*

Amylose exists in the crystal structures A, B, C, and V. The B-amylose, as in potato starch, is helical with an integral number of α-D-glucopyranosyl residues per turn. The configuration of amylose in solution has been debated for many years. The range of models in solution varies from helical (stiff, rod-like or loosely wound, worm-like) and interrupted helix to a random coil. The V-structure can occur after gelatinization of the starch, since amylose forms a complex with fatty acids, lipids and other polar molecules (Parker and Ring 2001).

The nowadays accepted models for A and B amylose structures are based upon 6-fold, left-handed double helices with a pitch height of 2.08-2.38 nm (Imberty et al. 1988; Imberty et al. 1991). In the B-type structure (Imberty et al. 1991), double helices are packed with the space group P6$_1$ in a hexagonal unit cell (a=b=1.85 nm, c= 1.04 nm) with 36 water molecules per unit cell. The symmetry of the double helices differs in A and B structures, since they have different repeating units (Imberty et al. 1991).

Potato starch contains between 18 and 21% amylose (Wurzburg 1986; Buléon et al., 1998) and the potato starches used in this work have been based on native potato starch with an amylose content of about 20% analyzed by size-exclusion chromatography (Svegmark et al. 2002). Due to its linear character, amylose can

crystallize and films of amylose thus have better barrier properties and show higher modulus than amylopectin films (Forssell et al. 2002; Rindlav-Westling et al. 1998, Rindlav et al. 1997).

3.2 Amylopectin

Amylopectin is a highly branched polymer and contains mostly α-D-1,4-anhydroglucose linkages along with α-D-1,6-anhydroglucose linkages at the branch points (*Figure 3.2*). The molecular weight of amylopectin is 10^6-10^8 Da (Whistler et al. 1984). Each branch contains 20 to 30 anhydroglucose units and the degree of polymerization is about 2 million units. The large size and branched nature of the amylopectin polymer reduces its mobility and prevents the polymers from becoming oriented close enough to permit hydrogen bonding. As a result, aqueous solutions of amylopectin are clear and resistant to gelling upon ageing.
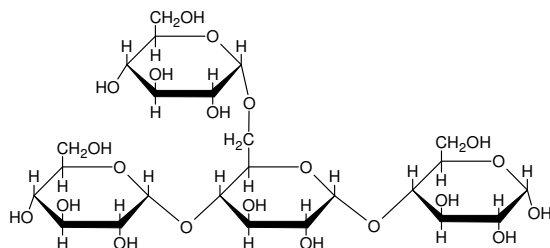
Figure 3.2. *The chemical structure of amylopectin.*

Amylopectin is usually assumed to support the framework of the crystalline regions in the starch granule. It has been shown that branching points do not induce extensive defects in the double helical structure (Imberty and Perez 1988; Buléon and Tran 1990).

The molecular structure of amylopectin is described by the cluster model first proposed by French (1972) and Robin et al. (1974). The cluster model generally accepted today (Hizakur 1986) is shown in *Figure 3.3*.

The crystalline and non-crystalline structures are major factors influencing the properties of the starch granules (Zobel 1988). The crystalline shells consist of alternating amorphous and crystalline lamellae which are approximately 9-10 nm thick (Jenkins and Donald 1995; Gallant et al., 1997).
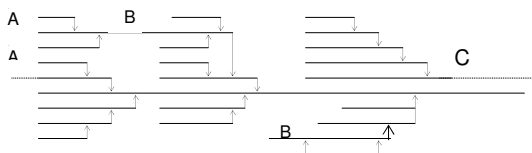
Figure 3.3. *Structure of amylopectin according to Hizakur (1986) where A-chains are associated with one cluster, B-chains with one to three clusters, and C-chains carry the reducing end group.*

There are three different types of crystalline structure (A, B, and C) for amylopectin within the crystalline lamellae (Figure 3.3). A-chains are associated with one cluster while B-chains are involved in one, two, or three clusters. A-chains are those that are linked to the rest of the molecule only through their reducing ends. B-chains are linked to the molecule through their reducing ends but, in addition, are branched at a C-6 position in one or more of their D-glucopyranosyl residues (Jenkins and Donald 1995). C-chains are those that bear the reducing end group. Potato starch has a B-crystalline pattern (Young 1984).

3.3 Phosphorus content and lipid content

Native starches contain small amounts of phosphorus (Gracza 1984). Potato starch contains 0.07-0.09% phosphorus covalently bonded to the amylopectin fraction in the monoester phosphate form. Koch et al. (1982) determined the phosphorus content of native potato starch to 0.083%, which corresponds to a degree of substitution of 4.36×10^{-3}. The starches used in the work reported in this thesis contain 0.06-0.29% phosphorus, with amylopectin potato starch having by far the highest content.

Potato starch contains only small amounts of lipids and proteins. The lipid content is very low, only about 0.06% and the protein content is also about 0.06% (Swinkels 1985).

3.4 Retrogradation

When using chemically modified starches, one has to be aware that they tend to retrograde rapidly. The retrogradation is a non-reversible process where the hydrated amylose molecules form hydrogen bonds between one another when the solution is cooled. The chains of amylose wrap around themselves as double helices, forming colloidal crystallites (Imberty et al. 1991). If the solution is dilute, particulate precipitation occurs whereas if the solution is more concentrated a network structure, a gel, is formed. The gel formation process in concentrated solutions is faster than the precipitation process in dilute solutions (Wurzburg 1986). The rate of retrogradation depends on several factors including starch concentration, degree of hydration, molecular weight, salt concentration, temperature, time and pH. Naturally occurring contaminants, like lipids (Godet et al. 1993a), can form inclusion complexes with the amylose molecule and initiate or speed up the retrogradation process. The retrogradation must not be confused with the phase separation induced by the interaction of hydrophobic functional groups. Such a phase separation in starches is fully reversible, whereas the retrogradation is a non-reversible process. The HM starches used in this work showed no retrogradation during the course of the experiments.

3.5 Modification of starches

Chemical modifications of various kinds can improve the functional properties of starch for different applications. *Table 3.1* shows the starches used in this work and the various modifications performed on the starches are described in the following sections. The HM starches are based on native potato starch and contain about 20% amylose, whereas the oxidized amylose potato starch contains about 70% amylose. The amylopectin potato starch is essentially 100% amylopectin.

_____

Table 3.1. *The different starches with the degree of modification where DS_N is the degree of substitution with respect to the hydrophobic part, i.e. the carbon chain, and X_{COOH} is the molar fraction with respect to the oxidized part.*

Starch	Label	X_{COOH}	Used in Paper	DS_N^a	DS_N^b	Net charge ($\mu eq/g$)
Ox. Amylose	OAM	0.021	II	n.a	n.a	- 550
HM. Amylopectin	HMAP	0.018	II	0.021	0.029	+ 52
Ox. Starch	Starch A	0.011	I, II	n.a	n.a	- 120
HM starch	Starch B	0.016	I, II	0.011	0.014	- 6.5
HM starch	Starch C	0.016	I, II	0.027	0.035	+ 105
HM. starch	Starch D	0.027	I, II, III	0.027	0.035	+20
HM starch	HONP	0.027	IV	0.027	0.035	+20
HP starch[c]	PONP	0.010	IV	n.a	n.a	n.a.

a) By Kjeldahl

b) By Dumas

c) HP starch was hydroxypropylated with DS of 0.011 in addition to the oxidation.

3.5.1 Oxidization

In industrial water-borne coatings applied at high shear rates the molecular weight of native starch has to be reduced in order to achieve sufficient low viscosity of the starch solution. This can commonly be performed by oxidation, which is a degrading process. Native starch has a very high viscosity at high starch concentrations whereas the viscosity of degraded starch is not greatly affected by an increase in concentration. This makes oxidized starch easier to use than native starch at higher concentrations. The oxidation process is mild and is performed under controlled conditions, and this allows the oxidant to attach to the most reactive bond on the starch polymer (Lehtinen 2000).

Sodium hypochlorite (Paper I-IV) first oxidizes the hydroxyl groups on the starch molecules to carbonyl groups and then further to carboxyl groups. The numbers of carboxyl and carbonyl groups on oxidized starch thus indicate the level of oxidation, at the hydroxyl groups at the C-2, C-3, and C-6 positions (Wurzburg 1986). When carboxylic groups are introduced into the starch, they sterically hinder the associative tendencies of the starch molecules and the starch solution has lower tendency to retrograde. In addition, in coating colors, the carboxylic groups help to prevent agglomeration of pigments under high shear conditions. Derivates that have an average of two or more constituent groups per glucose unit are considered to be highly substituted starches, while those having an average of 0.2 or less are

_____

considered to have a low degree of substitution (DS). The starches used in the work described in this thesis had a low degree of modification.

If the pH during oxidation is not correct, other compounds may form (*Figure 3.4*) but we have performed the oxidation under basic conditions which favor carboxylic acid formation.

The presence of carboxyl and carbonyl groups on starch sterically hinders associative tendencies (retrogradation) of starch molecules. This effect increases the stability of cooked starch slurries considerably, and accounts for the unique properties of the various grades of oxidized starches. The full effect of oxidation becomes apparent when the starch is cooked. The gelatinization temperature of the starch is reduced in proportion to the degree of oxidation. The granules disintegrate when cooked and this results in a reduction in the peak viscosity (Kearny and Maurer 1990). All these properties make oxidized starches suitable as paper coating binders and in addition, the anionic character of oxidized starches prevents agglomeration of pigments in coating formulations.
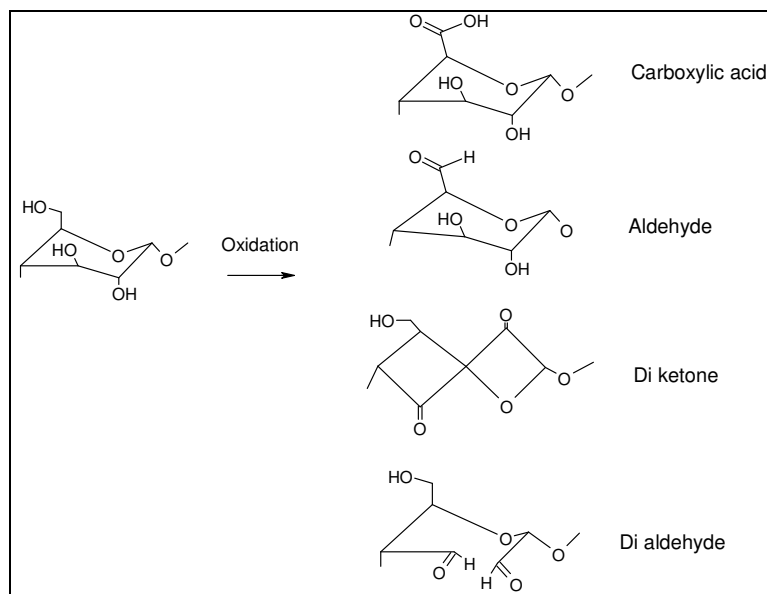
Figure 3.4. *Oxidation of starch. Hypochlorite favors the formation of carboxylic acid and aldehyde. At a basic pH carboxylic acid is mainly formed.*

3.5.2 Cationic starch ethers

The most widespread cationic starches are the tertiary amino derivatives which require an acidic environment to develop a strong cationic charge, and the quaternary amino derivatives which are inherently cationic and do not require protonation. Cationic potato starches are zwitterionic due to the presence of e.g. phosphate groups. The ionic repulsion of the cationic groups assists in dispersing the starch into the aqueous phase and contributes to the stability of the cooked starch. These changes in starch properties improve the efficiency of the starch as a binder: ionic bonds are formed between the cationic starch and the anionic pigment and fibers (Kearny and Maurer 1990).

In addition, the greater stability of the molecules in modified starches and their inherently better rheology make it possible to work with starches of higher molecular weights without runnability problems. This also leads to an improvement in the binding power of the starch (Glittenberg and Becker 1998). Cationic starches are formed by reacting starch with chemical reagents that add cationic substituent groups via ether linkages to glucose hydroxyl groups. Trimethyl-ammonium propyl chloride is a conventional wet-end additive for cationic starch in papermaking and it has a chemical structure similar to that of the chemical used for cationization in this work (*Figure 3.5*).

3.5.3 Hydrophobic starch

The starches used in this work were hydrophobically modified by reacting the pre-oxidized starch with a quaternary ammonium reagent similar to the reagent used for conventional cationic starches. The quaternary amine reagent (3-chloro-2-hydroxypropyl-dimethyl-dodecylammonium chloride), *Figure 3.5*, was added at an alkaline pH and ambient temperature (pH 11.3 and 37.5°C). When the reaction was completed, the pH was adjusted to 9.5. In this way, one positive unit charge was introduced per hydrophobic group.
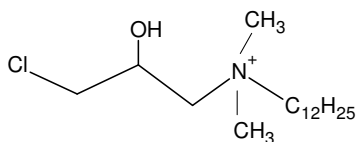
Figure 3.5. *Schematic sketch of the structure of the quaternary amine reagent.*

The reaction product was carefully washed with water in order to remove any remaining reagent and intermediates. The degree of substitution of hydrophobic/cationic groups was determined by analyzing the nitrogen content using Kjeldahl and Dumas methods. The Kjeldahl analyses were performed by the starch supplier, with the error range estimated by the supplier to be $\pm$ 4%. The resulting modified starches, which are amphiphilic, are shown in *Figure 3.6* and the characteristics of the starches used in this work are summarized in Table 3.1.
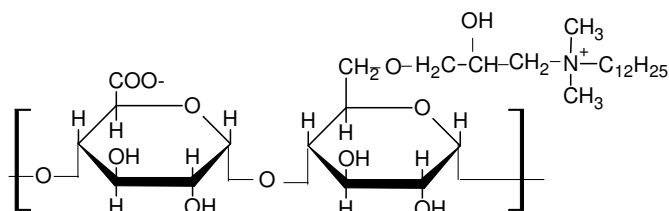
Figure 3.6. *Schematic sketch of the starch molecule after oxidation and hydrophobic modification.*

_____

3.5.4 *Hydroxypropylated starches*

The mechanism for the base-catalyzed reaction of propylene oxide with starch is considered to be of the substitutive nucleophilic bimolecular, or S_N2 type:

Starch-OH + NaOH → Starch-O⁻Na⁺ + H_2O [3.1]

Starch—O⁻Na⁺ + (epoxide) —CHCH₃ →(base) Starch—O ∕∖ CH₃ OH + NaOH

                                                                                                    [3.2]
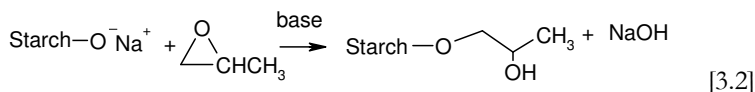
The reactive nature of propylene oxide is due to its highly strained three-member epoxide ring. Bond angles in the ring average 60° resulting in a very reactive molecule. The reaction kinetics is second order and dependent on the concentrations of the two reactants. Steric factors direct the reactivity to the less hindered (primary carbon) of the propylene oxide, resulting in the 2-hydroxypropyl starch derivative (Wurzburg 1986).

3.6   Cooking of starch

For starch to function at maximum efficiency as a binder in coating formulations in paper surface treatment, it must be fully dissolved and protected against retrogradation. Starch properties in solution are dependent on the cooking temperature, time and agitation. Higher temperatures, longer cooking times and the application of shear tend to effect a better dispersion (Kearny and Maurer 1990). Starch exists in units having a well-organized structure of closely associated and intermixed molecules (granules). These granules are insoluble in cold water. When heated in water to a certain temperature range, called the gelatinization temperature, these granular units are disrupted and they increase in volume by absorbing water. Hydrogen bonds holding the granules together are disassociated and the molecules begin to associate with water. The granular units finally disintegrate and, with continued heating beyond the gelatinization temperature, a starch solution is produced (*Figure 3.7*). The gelatinization is an endothermic phase transition.
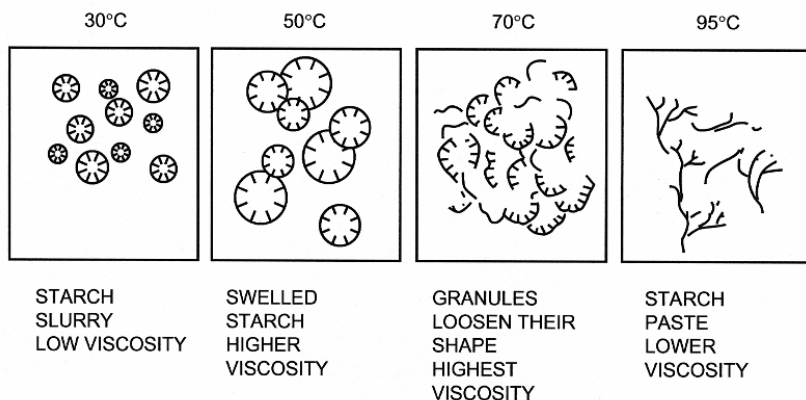
Figure 3.7. *Starch granules during cooking. Reprinted with permission from Fapet Oy, Helsinki Finland from 'Pigment Coating and Surface Sizing of Paper', Lehtinen (Ed).*

The gelatinization temperature for potato starch is in the range of 56-66°C. The granular organization and gelatinization are controlled by the major molecular component present, and the amylose content of the starch dominates this process. Under alkaline conditions, starch gelatinizes at lower temperatures.

The HM and amylopectin starches used in this thesis were prepared by cooking solutions in water bath of 95°C for 30 minutes under stirring, and then dilute with warm water to obtain the desired concentration The oxidized amylose was pre-heated in water bath at 95°C under stirring for 15 minutes, and then transferred to a pressurized steal compartment and held at 120°C for 15 minutes.

3.7   Inclusion complexes

The guest-host (inclusion complex) concept was first established by Cram, who received the Nobel Prize in 1987 together with Lehn and Pedersen for their work on these types of molecules. The guest-host concept describes the way in which a larger molecule, the host, forms a cave-like structure where a smaller molecule, the guest, can fit and a bond is created between them (Cram 1988).

The amylose molecule is known to be capable of forming helical inclusion complexes with a variety of organic substrates (Rundle and Edwards 1943; Mikus

_____

et al. 1946; Polaczek et al. 2000), lipids (Godet et al. 1995; Godet et al. 1993a,b; Eliasson and Kim 1995), alcohols (Chien et al. 1999; Nimz et al. 2004), iodine (Morrison and Laignelet 1983; Yamamoto et al. 1982; Immel and Lichtenthaler 2000) and other compounds.

X-ray diffraction analysis indicates a left-handed helix referred to as an α-helix. This helix is assumed to have a V-type crystal structure when forming a complex with aliphatic molecules (Karkalas and Raphaelides 1986; Helbert and Chanzy 1994). The amylose is the host molecule and wraps itself around the guest molecule. The number of glucose units in each turn of the helical coil is dependent on the size of the guest molecule. The host molecule is able to expand or contract around the guest (Biliaderis and Galloway 1989; Kubik et al. 1995).

A mixture of hydrophobically modified (HM), water-soluble, cationic cellulose ether and amylose dissolved together in water at high temperature and carefully cooled yields a solution having a viscosity higher than that of either polymer alone (Gruber and Konish 1997). This enhancement has been attributed to the formation of a cross-linked network where amylose forms a helical clathrate with the hydrophobic groups on the cellulose. Heating the complex results in extreme loss of solution viscosity, which then gradually rebuilds as the solution is re-cooled.

In Paper II, oxidized amylose starch (OAM) and hydrophobically modified amylopectin starch (HMAP) solutions were mixed together at different ratios at 80°C. Analyses were made to investigate whether inclusion complexes were formed between the HMAP and the OAM, as in the work of Gruber and Konish (1997). The rheological measurements (see section 5.5) showed results similar to those of Gruber and Konish, and the conclusion was that an inclusion complex between the two molecules may be formed. Differential scanning calorimetry (DSC) measurements of the starches in the presence of surfactants were investigated and endotherms confirmed the existence of inclusion complexes between the starch and the surfactants (see section 7.2). These endotherms indicate the possibility of inclusion complex when HM amylopectin was mixed with oxidized amylose.

4   SURFACTANTS

Surfactants have been extensively studied (see e.g. van Os et al. 1993). Surfactant is an abbreviation for surface active agent, i.e. an agent which is active at a surface. The surfactant contains two parts, a head group and a tail. (*Figure 4.1*)
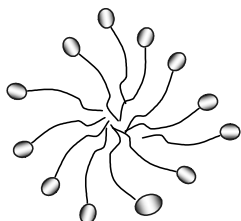

Figure 4.1. Schematic illustration of a surfactant molecule with a hydrophilic head group and a hydrophobic tail.

The head group of the surfactant is hydrophilic, i.e. it likes water and the tail is hydrophobic, i.e. it does not like water. This makes the surfactant amphiphilic, which means both hydrophilic and hydrophobic, each part of the surfactant being soluble in a specific fluid. The surfactant tail usually consists of hydrocarbon chains of various lengths and configurations. Depending on the nature of the head group, the surfactants are divided into ionic or nonionic, where the ionic surfactants can be either anionic or cationic. The anionic surfactants carry a negatively charged head group and the cationic a positively charged head group, while the non-ionic surfactants have no charge on their head groups (Jönsson et al. 1999).

A fundamental property of a surfactant is its ability to form aggregates in solution, so-called micelles. Micelles are formed at low surfactant concentrations in water. The concentration at which micelles start to form is called the critical micelle concentration, or CMC*,* and this is an important characteristic of a surfactant. The free surfactant concentration will never exceed the CMC, regardless of the amount of surfactant added to the solution. The two most common and most generally applicable techniques for measuring CMC are surface tension measurements and the solubilization of an otherwise insoluble compound.

In a micelle in water, the hydrophobic group of the surfactant is directed towards the interior of the cluster and the polar head group is directed towards the solvent (*Figure 4.2*). The resulting micelle is a polar aggregate highly soluble in water and with a low surface activity.

Figure 4.2. *Schematic illustration of a spherical micelle with the hydrophilic head groups on the outside and the hydrophobic tails inside the core.*

If a surfactant is adsorbed from an aqueous solution onto a hydrophobic surface, it normally orients its hydrophobic parts towards the surface and exposes its polar part to the water. The surface then becomes hydrophilic and the interfacial tension between the surface and water is reduced.
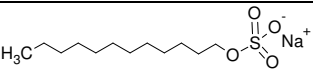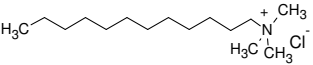
The CMC differs from surfactant to surfactant and depends on the surfactant's chemical structure, on the temperature, and pH, and on the presence of co-solutes like salts (Jönsson et al. 1999). Generally, ionic surfactants have a higher CMC than nonionic surfactants due to electrostatic repulsion (Lindman and Wennerström 1980); cationic surfactants have a slightly higher CMC than anionic surfactants and the CMC decreases with increasing alkyl chain length.

Anionic surfactants are used much more than other surfactants. One main reason for their popularity is their ease and low cost of manufacture. Anionic surfactants are used in most detergent formulations and the best effect is given by alkyl chains in the C12-C18 range.

4.1 Surfactants used in this work

The surfactants used in the work reported in this thesis were one anionic surfactant, sodium dodecyl sulfate (SDS), and one cationic surfactant, dodecyl trimethylammonium chloride (DoTAC). Their structures and CMC's are given in *Table 4.1*.

Table 4.1. Surfactants used in this work.

Surfactant	Structure	Abbreviation	CMC (mM)
Sodium dodecyl sulfate		SDS	8.1[a]
Dodecyl trimethyl-ammonium chloride		DoTAC	16[b]

[a] Jönsson et al. 1999, [b] Mukarjee and Mysels 1971

Even small portions of surface active compounds can affect the CMC of a surfactant. An example is a dodecyl alcohol contaminant in SDS, which is formed from hydrolysis of the surfactant. It is therefore of great importance that the SDS is handled carefully to avoid contamination of the surfactant solution.

4.2 Polymer-Surfactant mixtures

In a mixed solution of a surfactant and a HM polymer, there is a great tendency for association between the two cosolutes to occur. Extensive studies have been directed towards understanding the phase behavior of mixtures of cellulose derivatives and surfactants (Lindman et al. 1993; Thuresson et al. 1995). In the case of strong attraction between the two polymers, an associative phase separation occurs with one phase concentrated in the polymer and one in the dilute solution. High molecular weight of the polymer induces a higher degree of phase separation. In a polymer-surfactant system, the degree of polymerization of the micelle is not fixed as for polymers, but depends on the conditions like temperature, electrolyte concentration, etc.

A diblock copolymer and a polymer with pendant hydrophobic groups may show a self-assembly similar to that of a surfactant. An added surfactant will interact

strongly with the hydrophobic groups of the polymer, leading to a strengthened association between the polymer chains and thus to an increase in viscosity. The self-association of a HM, water-soluble polymer can be strengthened or weakened by a surfactant, depending on the stoichiometry and surfactant concentration. At low surfactant concentrations, a three dimensional network may be formed between the polymer and the surfactant giving rise to an increase in viscosity. As the surfactant concentration increases, the cross-links are broken and the network is destroyed, leading to a decrease in viscosity.

The associative properties of block copolymers and HM polymers have made them useful as thickeners in water-borne suspensions (Hester and Squire 1997). Beside the micelle-like type of associative behavior, a polymer that shows a coil-helix transition can act as a host molecule in inclusion complexes. This has been reported to apply to amylose in blends with HM cellulose ethers (Gruber and Konish 1997). The starches used in this work form inclusion complexes with surfactants, as discussed in Paper II. Many cellulose ethers show a reversible phase separation at higher temperatures and so do the HM starches in this work. This behavior is rare and is not predicted by the Flory-Huggins theory (see section 2.2).

The mixed micelle-like structures between surfactants and the hydrophobic polymer chains are formed above the critical association concentration (CAC) until the grafted hydrophobic chains are saturated with surfactant. This takes place at a surfactant saturation concentration (c_{sat}) which depends on the polymer concentration, molecular weight and hydrophobic modification, and on the temperature. The only self-assembled structures formed when the surfactant concentration is increased above c_{sat} are micelles binding only one hydrophobic polymer chain at a time (Jönsson et al. 1999; Piculell et al. 2001).

Non-ionic surfactants mixed with non-ionic polymers show a segregative phase separation (Jönsson et al. 1999). The introduction of charged groups strongly influences the phase separation phenomena and even a slight charge on either polymer or surfactant strongly enhances polymer-surfactant miscibility. Ionic surfactants tend to associate with non-ionic polymers. A mixture of two oppositely charged polyelectrolytes shows strongly associative behavior and there is a strong tendency for phase separation to occur (Jönsson et al. 1999).

_____

5   POLYMER RHEOLOGY

Rheology is the study of the flow and deformation of materials and a distinction is made between liquid, solid and viscoelastic materials.

To describe linear viscoelastic behavior it is useful to introduce mechanical models. Elastic materials, or solids, obey Hooke's law of elasticity and can be represented by a spring. The force on the element is proportional to the extension. Viscous materials on the other hand, or liquids, obey Newton's viscosity law and can be represented by a dashpot. The force on the element is proportional to the rate of extension. Viscoelastic materials are intermediates and exhibit both elastic and viscous properties simultaneously (Barnes et al. 1989).

5.1   Viscosity

When measuring viscosity, the shear stress created by the sample when the geometry is set to rotate is measured. The shear stress (σ) can be written as

$$\sigma = \frac{F}{A} \qquad\qquad\qquad [5.1]$$

where F is the force and A is the area of the sample (*Figure 5.1*).
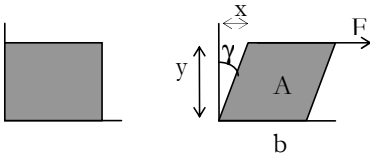
Figure 5.1. *Schematic representation of the parameters used in the definition of viscosity, a) before shear, b) after shear.*

The deformation of the sample, the shear strain (γ), depends on the movement in the x-direction and on the thickness of the sample. Often the time-derivative, the shear rate ($\dot{\gamma}$), of the shear strain is used to calculate the viscosity:

$$\eta = \frac{\sigma}{\dot{\gamma}} \qquad\qquad [5.2]$$

Results of viscosity measurements are commonly presented with viscosity as a function of shear rate. If a solution is Newtonian, e.g. a simple liquid like water, the viscosity is constant and independent of the shear rate. If the viscosity decreases with increasing shear rate, the solution is shear-thinning. In a shear-thinning sample, the structure is broken down faster than it is rebuilt and this causes the viscosity to decrease. When the viscosity increases with increasing shear, the solution is shear-thickening. Shear-thickening behavior is found in concentrated particle-containing solutions. When the viscosity decreases with time followed by a gradual recovery when the shear is ceased, the sample is thixotropic.

5.2 Viscoelasticity

A sample with both liquid-like and solid-like properties is viscoelastic. This behavior typically occurs in a semi-dilute or concentrated polymer solution. When the rheological properties of a viscoelastic sample are measured, an oscillating procedure is commonly used. During an oscillatory measurement, the non-stationary part of the rheometer geometry oscillates at constant frequency with varying amplitude (strain sweep), or at constant amplitude with varying frequency (frequency sweep). Oscillatory measurements are used for viscoelastic samples since they are non-destructive and the equilibrium properties of the sample are measured. The result is presented as the modulus, G, which is the ratio of the shear stress to the shear strain. The modulus can be divided into storage modulus, G', which represent the storage of elastic energy and the loss modulus, G'', which represents the viscous dissipation of energy (Larson 1999). The ratio G''/G' (called the loss tangent, $\tan\delta$) is high (>>1) for materials that are liquid-like, but low (<<1) for materials that are solid-like.

The complex modulus G^* is defined as

$$G^* = G' + iG'' \qquad\qquad [5.3]$$

where $i = \sqrt{-1}$. The magnitude of G^* is given by

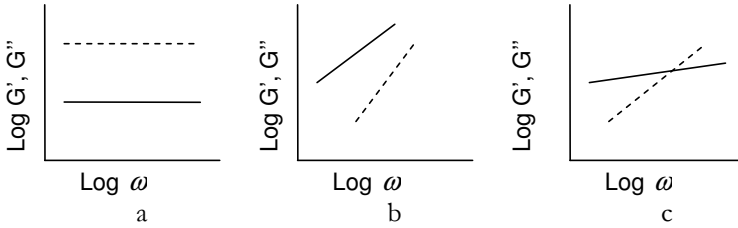$$G^* = \left(G'^2 + G''^2\right)^{1/2} \qquad\qquad [5.4]$$

The relation between complex viscosity (η^*) and modulus is given by

$$|\eta^*| = \frac{\left(G'^2 + G''^2\right)^{1/2}}{\varpi} \qquad\qquad [5.5]$$

where ω is the frequency of oscillation. The phase angle (δ) is thus defined as:

$$\delta = \arctan\left(\frac{G''}{G'}\right) \qquad\qquad [5.6]$$

The storage (G') and loss (G'') moduli for liquid-like and solid-like samples differ and are schematically shown in *Figure 5.2*.

Figure 5.2. *Schematic illustration of frequency-dependency of storage, G', and loss, G'', modulus for a) solid-like, b) liquid-like, and c) viscoelastic materials. The dashed line represents the storage modulus and the solid line represents the loss modulus.*

The storage modulus for elastic samples (solid-like) is independent of the frequency and larger than the loss modulus (Figure 5.2a). For viscous (liquid-like)

samples, the storage modulus is much lower than the loss modulus (Figure 5.2.b). For viscoelastic samples (Figure 5.2.c), the plots of storage and loss moduli versus frequency cross each other when the frequency increases (Barnes et al. 1989).

Viscoelastic measurements may be used to determine the gel point, as the crossover of the viscous and elastic responses ($G' = G''$), i.e. where the phase angle is 45° (Paper I). If the phase angle falls to a value close to zero, this indicates the formation of an elastic network structure (Svegmark and Hermansson 1990).

5.3   Measuring geometries

Several methods are available for measuring the rheological properties of a solution, but the geometry of the measurement device is of great importance. Several different measurement geometries exist, and the ones used in this work are shown in *Figure 5.3*.
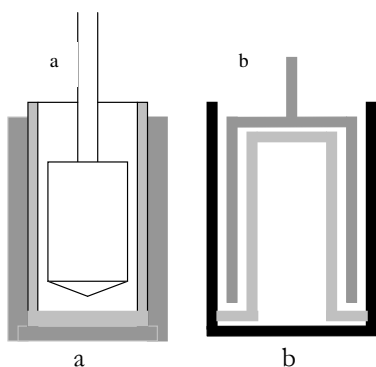
Figure 5.3. Schematic illustration of the rheometer geometries used in this work, a) Concentric cylinder and b) Double gap geometry.

The concentric cylinder geometry (Figure 5.3a) was used for solutions of medium viscosities. The liquid sample is transferred to the cylinder and the bob is inserted into the liquid. In this geometry, the bob oscillates while the cylinder is stationary. The double-gap geometry (Figure 5.3b) was used for solutions with low viscosity,

_____

close to the viscosity of pure water. Two other common geometries that are not discussed here are the cone and plate, and plate and plate geometries.

5.4   Rheology of starch solutions

The rheological properties of the hydrophobically modified (HM) starch solutions were investigated (Paper I) by temperature sweeps at constant frequency and strain (within the viscoelastic region, determined by amplitude sweep). For starch properties, see Table 3.1 (page 16).

Figure 5.4 shows the complex viscosity ($|\eta*|$) as a function of temperature measured during a cooling and reheating loop at continuous oscillatory shear. A clear hysteresis loop in complex viscosity was observed at high concentrations of the starches, but the process was reversible. The complex viscosity obtained on cooling was always lower than the corresponding value obtained on re-heating.
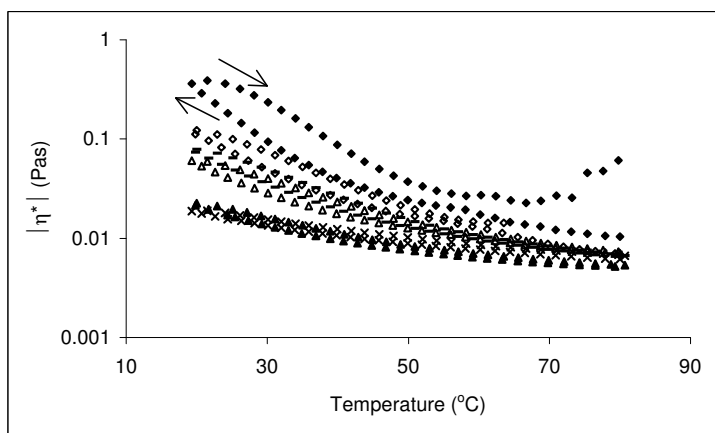
Figure 5.4. *Complex viscosity as a function of temperature for different starches and concentrations at pH=8.* **Starch C**: *8.9 wt % (♦), 7.8 wt % (◇), 6.5 wt % (-);* **Starch B:** *7.6 wt % (△), 6.0 wt % (▲), and* **Starch A**: *9.2 wt % (✕). The arrows indicate the temperature loop for Starch C at 8.9 wt %.*

When subjected to a cooling ramp, the complex viscosity of Starch C started to increase rapidly at about 45°C, but Starch B and Starch A showed a somewhat

lower temperature effect. The complex viscosity of Starch B and Starch C at high concentrations (above 8 wt-%) increased with decreasing temperature, indicating the formation of a gel network in combination with the normal viscosity-temperature behavior of a polymer solution, i.e. the Arrhenius behavior. The difference in $|\eta*|$ indicated differences in gelation behavior. Oxidized Starch A showed similar behavior, but only Arrhenius behavior was present since the increase in viscosity was not as pronounced as that of Starches B and C (Paper I).

The onset temperatures for the drop in phase angle from 90° are shown in *Figure 5.5*. A clear hysteresis loop in phase angle was observed at high starch concentrations. The concentration-dependence of the gel network formation seems to be quite large. At lower concentrations, the phase angles decreased only slightly but at higher concentrations the decrease in phase angle became more pronounced. The overlapping concentration, c^*, was determined to be about 3.5 wt% (pH 8, 20°C) for all molecules in the starch solution and this was lower than the concentration at which δ started to decrease with temperature and $|\eta*|$ started to increase with temperature (Starch A, Paper I).
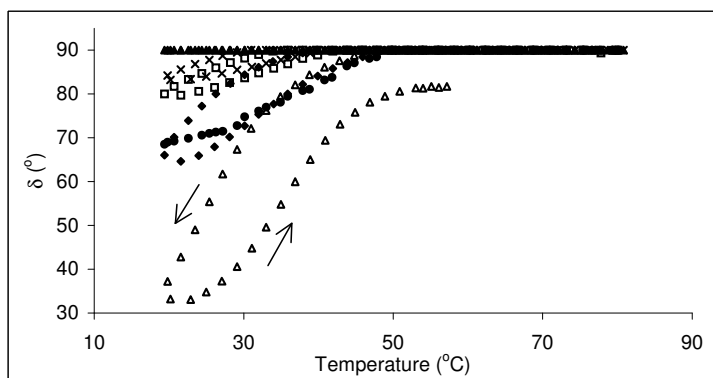
Figure 5.5. Phase angle, δ , as a function of temperature at pH =8. **Starch C:** 12.1 wt% ($\triangle$), 6.5 wt % ($\square$), **Starch B:** 12.2 wt % ($\blacklozenge$), 7.6 wt % ($\times$), 6.0 wt % ($\blacktriangle$), **Starch A:** 9.2 wt %($\bullet$). The arrows indicate the temperature loop for Starch C at 12.1 wt%.

It is evident in Figure 5.4 that the HM Starch C showed a large increase in complex viscosity with increasing starch concentration. The increase in complex viscosity

for Starch B after cooling without oscillatory shear was similar to that observed for Starch A and could be explained as an Arrhenius effect. However, when the starches were cooled during oscillation, the complex viscosity at room temperature of Starch B was substantially higher than that of Starch A. In conclusion, a zero net charge on the amphoteric starch promoted a reversible precipitation (Starch B), while a positive net charge led to the formation of a gel network upon cooling (Starch C). In both cases, the phase separation and gel formation were dependent on the polymer concentration.

5.5   Inclusion Complex Determined by Rheology

Gruber and Konish (1997) showed that a combination of hydrophobically modified (HM), water-soluble, cationic cellulose ether and amylose dissolved together in water at high temperature and carefully cooled yielded a solution with a viscosity higher than that of either polymer alone. This enhancement was attributed to the formation of a cross-linked network with amylose as a helical clathrate with the hydrophobic groups as guest. Upon heating, the increase in viscosity due to network formation was lost, but it was gradually recovered when the sample was cooled.

The complex viscosity of the mixtures of oxidized amylose (OAM) and hydrophobically modified amylopectin (HMAP) was measured at a constant frequency and constant temperature (Paper II). *Figure 5.6* shows the complex viscosity as a function of wt% OAM at 20°C.

The complex viscosity increased with increasing amount of amylose and a peak was observed at 25 wt% amylose (of the total weight of the mixture). The increase in viscosity may be attributed to the formation of an inclusion complex between the OAM and the HMAP where OAM acts as host and the hydrophobic alkyl chain on the HMAP is the guest. This is consistent with prior observations of inclusion complexes between e.g. amylose and lipids (Godet et al. 1993a).

_____
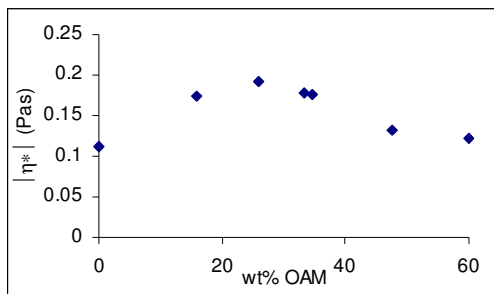
Figure 5.6. *Complex viscosity of the inclusion complex solution at 20°C as a function of the amount of oxidized amylose expressed as a weight percentage. The concentration of the starch solution was 12 wt%, the strain 1.0 and the frequency 1.0 Hz.*

At low temperatures or in appropriate solvents, starches adopt a helical conformation (Godet et al. 1993a; Whistler et al. 1984). At high temperatures, it is increasingly possible that the bond angles and the dihedral angles deviate from values compatible with the helix, and that the amylose fraction (e.g. OAM) undergoes a helix-coil transition. Long amylopectin chains (e.g. HMAP) also possess some ability to form helices. The forces promoting the formation of a helix are due to hydrophobic interactions. Consequently, a hydrophobic interaction between the starch and the hydrophobic tail can create a three-dimensional network which will give rise to an enhanced viscosity.

6 TURBIDITY, PARTICLE SIZE AND YIELD OF PRECIPITATION

The temperature-responsive starch solutions used in this work phase separate upon cooling. When freshly cooked, the warm starch solution is a clear liquid. As the solution starts to cool to room temperature, the solution becomes more turbid and the liquid becomes cloudy or milk-like. Phase separation of a starch solution creates a turbid system. The scattering of light and the turbidity depend strongly on the particle size (Gregory 1985).

6.1 Turbidity

The turbidity of a solution can be measured in different ways. In this work, UV spectroscopy was used to give information about the light scattering of the solution (Paper I, Paper II, Paper III, and Paper IV).

Figure 6.1 shows a beam of parallel radiation before and after it passes through a solution of concentration c (M) and cuvette thickness L (cm) (Skoog and Leary 1992). As a consequence of interactions between the photons and absorbing particles as well as scattering by large particles, the power of the beam is attenuated from I_0, incident light intensity, to I, outgoing light intensity.
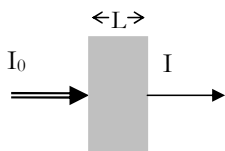
Figure 6.1. Attenuation of a beam of radiation by an absorbing solution.

The transmittance (T) of the solution is the fraction of the incident radiation transmitted by the solution

$$T = \frac{I}{I_0} \qquad\qquad [6.1]$$

The turbidity (τ) can be calculated from the transmittance (T) according to

$$\tau = -\frac{(\ln T)}{L} \qquad\qquad [6.2]$$

The turbidity depends on the concentration and light scattering properties of the particles (Gregory 1985). For a monodisperse suspension containing N particles per unit volume, the turbidity is expressed as

$$\tau = NC \qquad\qquad [6.3]$$

where C is the scattering cross section of a particle. The scattering cross section gives the dimensionless scattering coefficient, Q, which for spherical particles with the radius a is

$$Q = \frac{C}{\pi a^2} \qquad\qquad [6.4]$$

The value of Q depends greatly on the wavelength of the light and on the size and refractive index of the particles. For very small particles, < 10% of the light wavelength, Rayleigh theory applies while for much larger particles Q approaches the value 2. It is shown in the literature (Gregory 1985) that for small particles, Q increases rapidly with increasing particle size and then passes through a series of regularly spaced maxima and minima, ultimately approaching the value $Q = 2$. If plotting the specific turbidity (turbidity divided by the volume fraction of particles) as a function of particle diameter, a sharp rise in specific turbidity is often observed at a certain range of particle sizes. As a consequence, the turbidity of a given suspension should change markedly as changes in particle size occur, for instance as particles aggregate.

It is extremely important that the solution is homogeneous when the turbidity is measured by light scattering. If a large portion of the solution precipitates, the heavy particles fall to the bottom of the cuvette and the turbidity measurement is incorrect since the particles packed on the bottom will not contribute to the scattering of the light beam. All measurements made in this work were performed immediately after stirring the sample well.

The transmittance of the freshly prepared starch solutions was measured on a conventional UV-spectrophotometer (Shimadzu, UV2101 PC, Japan). Each sample was run in a cycle from 80°C to room temperature and back to 80°C (Paper I). Surfactant-starch-water and starch-water samples were measured at 23°C to investigate whether the surfactants had any stabilizing effect on the starch in solution (Paper II). Measurements were performed on HONP of different pH (at 23°C) and the effect on turbidity upon addition of glycerol was also investigated (Paper IV).

6.1.1 Results – turbidity

The solution of Starch B in water showed an increase in turbidity (τ) with decreasing temperature, indicating that phase separation occurred at low temperatures (Paper I). The solution of Starch C showed an increase in turbidity with decreasing temperature, but the increase in turbidity in this case was much weaker than for Starch B. The turbidity of starch A was unaffected by the temperature (*Figure 6.2*).
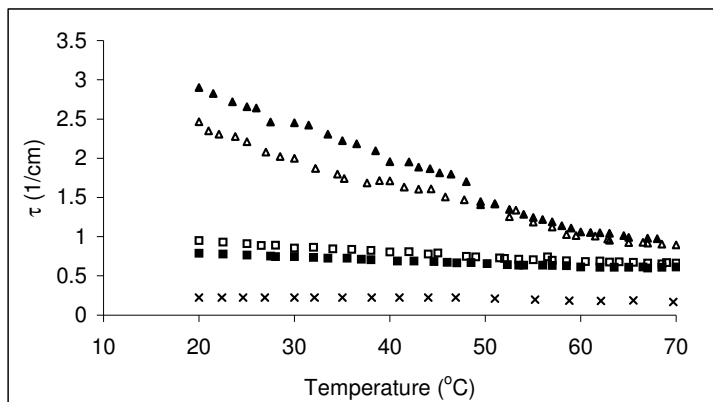
Figure 6.2. *Turbidity cooled from 80 °C to room temperature, as a function of temperature for different starch grades at pH=8. Starch B: 4.7 wt% (▲) and 7.6 wt% (△); Starch C: 7.8 wt% (■) and 4.6 wt% (□); and Starch A: 8.2 wt% (✕).*

Starch B showed a rapid increase in turbidity with decreasing temperature. At a given temperature, the solution with a lower starch concentration showed a higher turbidity than the solution with a higher starch concentration. Precipitation occurred more readily at low starch concentration, which is similar to the observed retrogradation of unmodified starches where a gel is formed in concentrated solutions and a solid precipitate is formed in dilute solutions (Wurzburg 1986). In all cases, the turbidity behavior was reversible. Thus, retrogradation cannot be the explanation of the phase separation. Precipitation occurred to a greater extent with Starch B than with Starch C. Starch C had a higher net charge density than Starch B (almost zero net charge), and the net charge density on the starch was important for the phase separation behavior; high charges promoting smaller driving forces for the particles to be close to each other and form aggregates.

The turbidity of the starch solutions was also measured in the presence of surfactant (Paper II). It was observed that the turbidity increased upon cooling for Starch D (highly substituted, almost zero net charge) both in the presence and in the absence of surfactant. At room temperature, a white precipitate was formed with Starch D in the absence of surfactant. When a cationic surfactant (DoTAC) was added to the starch, the turbidity was considerably lower and, with an anionic surfactant (SDS), the turbidity decreased by one order of magnitude. The

difference in turbidity compared to that of pure starch solution indicates that the surfactant stabilized the starch and prevented phase separation.

Similar results were obtained with Starch C (highly cationic) in the presence of SDS. The turbidity was two orders of magnitude lower than with pure Starch C and did not change with temperature in the presence of SDS. When DoTAC was added, the turbidity was one order of magnitude lower than that of the pure starch and the turbidity did not change over the temperature range measured. It seemed that SDS stabilized Starch C and prevented precipitation better than DoTAC. This stabilization effect was probably due to the formation of mixed micelles between the pendant hydrophobe and the added surfactant on the starch surfaces.

The turbidity was measured on HONP at different pH levels and with addition of glycerol. It was observed that the turbidity was highest for the sample with a pH of around 10 (*Figure 6.3*), the pH that gave the largest amount of precipitate (section 6.2). When the pH was further increased, the turbidity again decreased. The samples containing glycerol gave similar results as the solution with the same pH (pH 6.9).
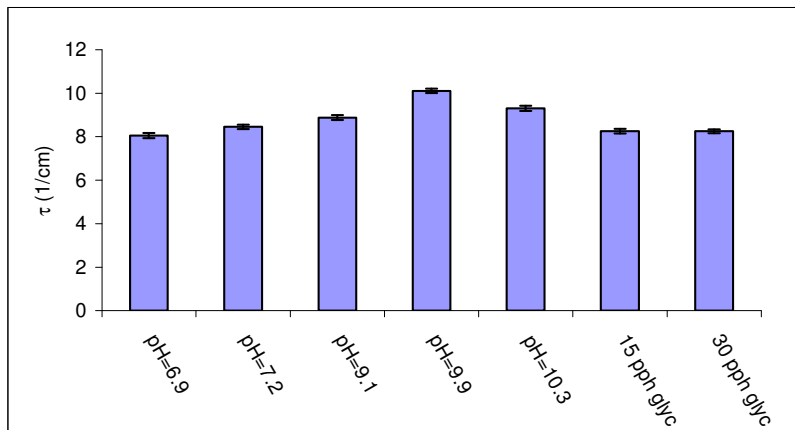
Figure 6.3. *Turbidity of HONP solutions at 23 °C of different pH at 550 nm and with addition of 15 and 30 pph glycerol (pH 6.9).*

6.2 Precipitation Yield

The precipitation yield was determined gravimetrically after separation of the solid phase by centrifugation (Paper I, Paper III and Paper IV). For starch solutions with initial concentrations of 10 wt%, the precipitation yield was 15% for Starch and 4% for Starch C (pH 8, 23°C).

For HONP (Paper III and Paper IV) the yield of precipitation was determined gravimetrically at different pHs and the results are summarized in *Table 6.1*.

Table 6.1. *The pH and the precipitation yield of HONP (Starch D), measured gravimetrically after cooling to room temperature followed by centrifugation.*

pH	Yield (%)
3.3	7.6 ± 0.2
6.5	8.2 ± 0.2
7.2	11.2 ± 0.1
9.1	14.9 ± 0.3
9.9	15.8 ± 0.2

It was observed that the precipitation yield increased with pH up to pH 10 and it was concluded that the optimal pH for a high precipitation yield was about 9.9; this pH was chosen for isolation of the particulate material (Paper IV). Addition of glycerol seemed to partly inhibit the precipitation since the yield was only 6.4% at pH 6.9 after addition of 15 pph glycerol compared to 8.2% at the same pH without glycerol.

The precipitated phase and the supernatant after phase separation were analyzed with respect to their nitrogen content (Paper IV). The analysis, performed by Dumas method, showed that the precipitated phase contained a substantially higher amount of nitrogen, e.g. hydrophobic groups. The degree of substitution of nitrogen groups were 0.035 for HONP before phase separation, 0.056 for the precipitated phase and 0.028 for the starch remaining in the supernatant.

6.3 Particle size

The particle size distribution was measured after separating the precipitate and re-dispersing the solid phase in water on a Coulter LS130 Fluid Model (Coulter

Electronics Ltd., Luton, England) at a starch concentration of about 0.1%. Distilled water was used as fluid medium. The mean particle size of Starch B was 20 μm (Paper I). Järnström et al. (2000) reported that the mean particle size of precipitates formed from solutions of starch similar to Starch B and Starch C was slightly above 1 μm. The larger particle size observed in the present investigation indicates that the DS and the rate of cooling may affect the precipitation process.

6.4   Charge density

The charge density of the starches was measured using a Particle Charge Detector (Mütek, PCD 03, Herrsching Germany) at pH 8. The anionic starch was titrated with poly (diallyldimethylammonium chloride) [CAS No. *26062-79-3*] and the cationic starch was titrated with polyethylene sodium sulphonate [CAS No. *25053-27-4*]. The HM starches were amphiphilic and amphoteric/zwitterionic. The charge of the starches was dependent on the pH, since the carboxyl and phosphate groups protonate at different pHs. The charges of the HM starch used in this work are summarized in Table 3.1 (page 16).

7 MATERIAL CHARACTERIZATION

It is well known that amylose can form helical complexes with a variety of substance, including lipids, surfactants and aromatic compounds. Several experimental procedures including NMR and DSC, have been used to determine the helical transition, but in the present work NMR was used only to characterize the starch and not to gain information about inclusion complexes.

7.1 ^{1}H-Nuclear Magnetic Resonance Spectroscopy

Liquid nuclear magnetic resonance (NMR) is a useful tool for revealing the molecular structure of a material. The technique is based upon the measurement of the resonance in the radio frequency region (about 400 to 600 MHz) of a nucleus exposed to a magnetic field (Skoog and Leary 1992). In contrast to ultraviolet, visible, and infrared absorption, the nuclei of the atoms are involved in this absorption process. Atomic nuclei have a quantized spin angular momentum (a magnetic moment) and they can interact with a magnetic field (Skoog and Leary 1992). This was first proposed by Pauli in 1924 but it was not until that Bloch and Purcell independently showed experimentally that a nucleus absorbs electro-magnetic radiation in a strong magnetic field as a consequence of energy level splitting induced by the magnetic field. Bloch and Purcell received the Nobel Prize in 1952 for their work. NMR spectroscopy uses the fact that nuclei of the same kind in a molecule resonate at different frequencies, if they are surrounded by different electronic environment.

Starch has been extensively investigated by NMR in the literature by proton (^{1}H), carbon (^{13}C), and phosphorus (^{31}P), of all which have the spin quantum number 1/2 (Williams and Fleming 1995; Nilsson et al. 1996; Gidley 1985). Simple one-dimensional ^{1}H-NMR spectra give information of the glucosidic linkages in starch as the protons on the anhydroglucose units resonate in a typical frequency range.

_____

The high resolution of ^{1}H-NMR spectrometers enables the different anomeric protons (H-1) of starch to be separated sufficiently, to distinguish between the α-(1→4) and α-(1→6) linkages (*Figure 7.1*) (McIntyre 1990; Gidley 1985). The peak area of the signal is proportional to the number of protons and both qualitative and quantitative information is obtained (Skoog and Leary 1992). Nilsson et al. (1996) showed that ^{1}H NMR spectroscopy is a sensitive, direct method for determining the degree of branching and average chain length of starch. It has also been used to determine the molar substitution of hydroxypropylated starch and ^{31}P-NMR has been used to determine the positions of the phosphate groups on the glucose units in potato amylopectin (Muhrbeck and Tellier 1991).

### 7.1.1   Results – ^{1}H NMR

A homogeneously dissolved sample is essential if well resolved NMR signals are to be obtained. D_2O has generally been used as a solvent for NMR-samples of starch and starch-related polysaccharides (Gidley 1985). In the present work (Paper II), potato, amylose and amylopectin starch were dissolved in D_2O at 80°C, followed by freeze-drying. The freeze-dried, deuterated sample was dissolved in D_2O (20 mg/ml), heated to 80°C and never cooled below 70°C before analysis to prevent retrogradation and phase separation of the starch samples. ^{1}H NMR measurements were performed with a Bruker 500 MHz spectrophotometer (mod. ARX500, Bruker Fällanen, Switzerland) and spectra were accumulated at 80°C using D_2O as solvent and the solvent peak for reference. The resulting NMR-spectrum for HM potato starch (Starch D, Paper II) is shown in *Figure 7.1*. The degree of branching was calculated according to

$$\text{Degree of branching} = \frac{(\text{integral } H-1(1 \rightarrow 6))*100}{\text{integral } (H-1(1 \rightarrow 4) + H-1(1 \rightarrow 6))} \qquad [7.1]$$

which expresses the number of branching points compared with the total number of linkages. The average chain length, CL, was calculated by

$$\text{Average Chain Length} = \frac{\text{integral } (H\text{-}1(1 \rightarrow 4) + H\text{-}1(1 \rightarrow 6))}{\text{integral } (H\text{-}1(1 \rightarrow 6))} \qquad [7.2]$$
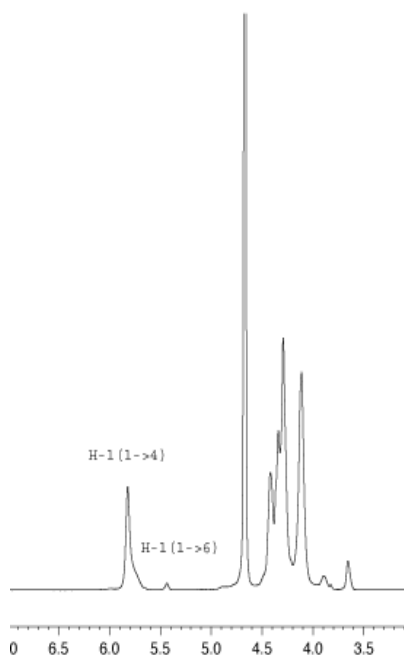
Figure 7.1. *^{1}H NMR spectrum of HM potato starch (20 mg/ml in D$_2$O, 80 °C).The degree of branching was 4.5 % and the average CL was 22.4.*

The ^{1}H NMR spectrum showed one peak assigned to the 1→ 4 linkages and one peak assigned the 1→ 6 linkages for Starch A, Starch D and HMAP (see Figure 2, Paper II). In OAM, there was only one 1→ 4 linkage peak since amylose is mainly linear. The degree of branching of the starches was calculated using equation [7.1]. The degree of branching was 4% for Starch A, 4.5% for Starch D and 4.9% for HMAP. Nilsson et al. (1996) reported that degraded amylopectin starch from potato had a degree of branching of 4.3%, which agrees with the obtained results in the present work. OAM had an average chain length of 100 (linear) while Starch A had 24.9, Starch D 22.4 and HMAP 20.6. The degree of branching reflects the CL in the starch sample, since each amylopectin chain has one branching point. The average values for fractionated (separated) amylopectin from potato starch have been reported to be 19-24 (Gidley 1985), and the values obtained in this work agree well with the figures found in the literature.

7.2 Differential Scanning Calorimetry

Differential scanning calorimeter (DSC) analysis involves the measurement of the heat flow associated with transitions in materials as a function of time and temperature in controlled atmosphere (Gmelin 1997). In a DSC measurement, a reference sample is subjected to the same conditions as the material of interest and the difference between the reference and the sample is measured while a temperature change is applied to the system.

The melting transition, *Tm*, is a first-order transition. It is characterized by its baseline and the endotherm of the process. *Tm* of a polymer is usually indicated by a broad endothermic melting peak. Melting is an equilibrium study and defined as the intersection of the free enthalpies at equilibrium. At *Tm* the free energy is zero and *Tm* only depends on the heat of fusion and the entropy of fusion (Turi 1997).

A glass transition appears as a shift in the horizontal base line (*Figure 7.2*) and arises from the onset of translational and/or rotational motion in highly disordered materials. It is a second-order transition. The change in base line at the glass transition temperature, *Tg*, underscores the importance of the *Tg* as a material property since it clearly shows the substantial change in rigidity that the material experiences within a short temperature span (Turi 1997).

The total heat flow measured by the calorimeter can be expressed by the first law of thermodynamics

$$\frac{dH}{dt} = C_p \frac{dT}{dt} + f(T,t) \qquad\qquad [7.3]$$

where dH/dt is the total heat flow, C_P is the specific heat capacity, dT/dt is the underlying heating rate and $f(T,t)$ is the kinetic response of the sample.
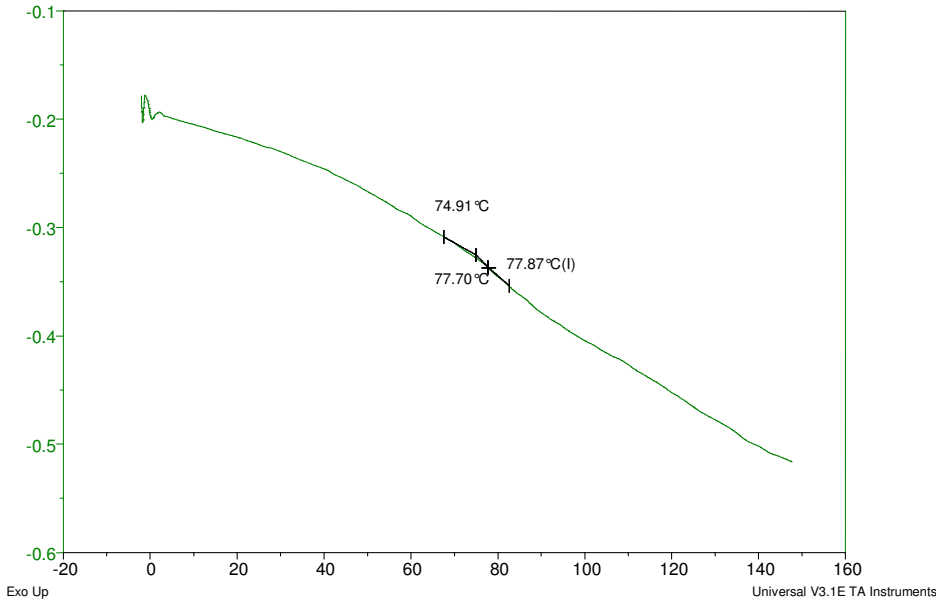
Figure 7.2. *DSC thermogram and Tg determination of HONP starch heated in modulated mode.*

Modulated DSC (MDSC) is an extension of linear DSC and utilizes a modulated heating program that permits the separation of overlapping thermal events and thus provides a more precise basis for the interpretation of the results (Weyer et al. 1997). The principle of MDSC is to superimpose a sinusoidal heating rate (modulation) over the traditional linear heating rate. This causes the average sample temperature to change continuously with time. The sinusoidal heating rate gives the heat capacity in MDSC operations and is called the reversing heat flow. The total heat flow signal measured in MDSC is both qualitatively and quantitatively equivalent to the heat flow signal from a standard DSC at the same average heating rate. The glass transition temperature is an example of a heat capacity transition and it appears in the reversing heat flow curve (Figure 7.2). The measured value of *Tg* depends on the heating rate, and a lower heating rate gives a lower apparent *Tg* (Kan 1999). The non-reversing heat flow gives the enthalpic relaxation, the crystallization and the melting.

In the work reported in this thesis, the heat flow of the sample (Paper II) and the glass transition temperature, Tg, (Paper IV) were measured with a differential scanning calorimeter (DSC), DSC 2920 CE, TA Instruments, New Castle, in the modulating mode (MDSC). The measured Tg and the theoretical Tg have been compared in Paper IV. The theoretical Tg (Tg_c) is given by

$$Tg_c = \sum Tg_i w_i \qquad\qquad\qquad [7.4]$$

where Tg_i is the glass transition temperature of component i and w_i is the concentration by weight of component i (Stevens 1999). Tg should decrease with increasing glycerol content in the films. Orford et al. (1989) approximated the $Tg's$ of dry amylose and amylopectin to 227°C and, based on extrapolations Bizot et al. (1997) determined the dry starch transition to be 316°C. The following values of Tg for pure components were used in the calculations: Tg = -85°C for glycerol (Champeney and Kaddour 1984), Tg = -137°C for water (Velikov et al. 2001) and Tg = 124°C for starch films. The Tg for the starch film, 124°C (Paper IV), was calculated by equation [7.4] by using Tg = 90°C for a starch film with 13% moisture (Lourdin et al. 1997; Stading et al. 2001).

7.2.1 Results – DSC

In Paper II, DSC studies were carried out to investigate the presence of an endotherm indicating inclusion complexes between starch and surfactant. Different starches were investigated in the presence of two surfactants: DoTAC (cationic) and SDS (anionic). When Starch D (slightly cationic) was heated in the presence of cationic DoTAC, an endotherm was observed between 95°C and 120°C indicating the presence of a starch-surfactant inclusion complex. For pure samples of Starch D a broad endotherm was observed between 45°C and 60°C. This broad endotherm vanished when starch was heated in the presence of the cationic surfactant, indicating that the surfactant stabilizes the starch solution.

In the case of Starch C (highly cationic), no peak was observed in the presence of cationic surfactant, indicating that no starch-surfactant inclusion complex was

formed. This may be explained by repulsive effects on complex formation, since the starch and surfactant have similar charges.

In the presence of SDS (anionic), all the starches showed an endotherm around 95°C which was attributed to the starch/surfactant inclusion complex (*Figure 7.3*). This endotherm agrees with those observed for starch/lipid systems (Eliasson 1994). The DSC measurements indicate that Starch C forms a complex with SDS but not with DoTAC, while Starch D forms a complex with both surfactants. One possible explanation may be strong electrostatic stabilization of the highly cationic Starch C in the presence of cationic surfactant.
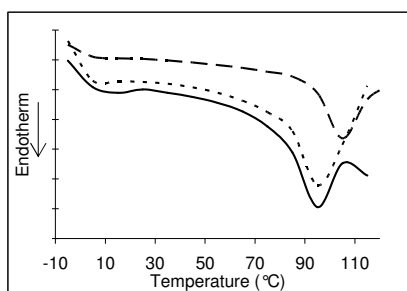
Figure 7.3. *DSC endotherm of* different starch grades in the presence of SDS for Starch A (- - -), Starch C (··) and Starch D (—) (*Paper II).*

Tg was measured on films of different starch grades. The DSC measurements on all the free films (Paper IV) showed a decrease in *Tg* with increasing glycerol content (*Table 7.1*) indicating an increasing degree of plasticization. The PONP films had the highest *Tg* in the absence of glycerol. *Tg* was similar for all films containing 30 pph glycerol, and there was good agreement between the experimental and theoretical *Tg* values.

**Table 7.1.** *Measured and theoretical Tg for different starch films with different glycerol contents.*

Sample	Glycerol (pph)	Moisture (%)	Tg measured (°C)	Tg theoretical (°C)
PONP	0	14.8	85.0 ± 1.6	85.3
	15	10.6	71.8 ± 2.3	69.1
	30	11.9	47.3 ± 1.6	44.6
HONP	0	12.9	78.5 ± 0.5	90.4
	15	11.6	57.8 ± 3.5	66.6
	30	12.0	44.7 ± 0.1	44.4
HONP$_S$	0	13.5	81.2 ± 0.4	88.8
	15	10.9	58.6 ± 3.8	68.3
	30	11.7	44.1 ± 0.5	45.1

Tg of starch films increases with increasing crystallinity (Stading et al. 2001) of starch. Thus, the fact that *Tg* decreased with increasing amounts of glycerol, as observed for the free films (Paper IV), indicates a decrease in crystallinity of the films. Myllärinen et al. (2002a) showed that amylose films with 10% glycerol had 23% crystallinity when stored for seven days at 54% RH, and 32% crystallinity when stored at 91% RH. The increased crystallinity was due to ordering of the B-type structure with water uptake of the films. Fresh amylose films in the dry state (stored over P_2O_5) had 6% crystallinity. Further, Myllärinen et al. (2002b) showed that glycerol was less effective as a plasticizer than water.

8 SURFACE ANALYSIS

8.1 Contact angle

Contact angle measurements were first described by Thomas Young in 1805 (van Oss 1994) as a technique to determine the interaction energy between a liquid (L) and a solid (S) (*Figure 8.1*).
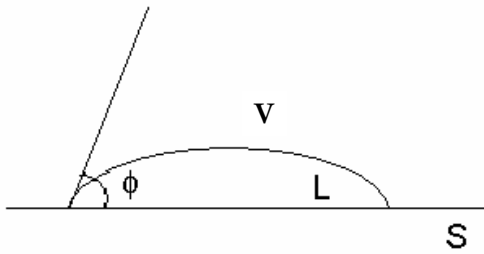
Figure 8.1. *Drop of liquid on a solid; S is the solid, L is the liquid, V is the vapor, and ϕ is the contact angle.*

Contact angle measurements are performed by placing a drop of liquid with known surface energy on the surface. The contact angle ϕ is measured at the tangent to the drop, starting at the triple point solid-liquid-vapor. The contact angle is a measure of the resultant of the energy of cohesion of the liquid and the energy of adhesion between liquid and solid (*Figure 8.2*) where the subscripts SV, SL, and LV refer to the solid-vapor, solid-liquid, and liquid-vapor interfaces, respectively.

Young gave the following equation

$$\gamma_{SV} = \gamma_{SL} + \gamma_{LV}\cos\phi \qquad\qquad [8.1]$$

The last term on the right-hand side in equation [8.1] is the projection of the vector γ_{LV} on the plane of the surface. For complete spreading of the drop onto the surface, the following criteria must be fulfilled: $\gamma_{SV} - \gamma_{SL} > \gamma_{LV}$, and then $\cos\phi = 1$.
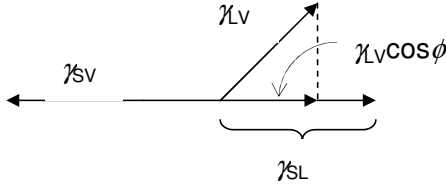
Figure 8.2. *Complete resolution of forces about a three-phase base line where the subscripts SV, SL, and LV refer to the solid-vapor, solid-liquid, and liquid-vapor interfaces, respectively.*

Figure 8.3 illustrates the difference between a hydrophilic and a hydrophobic surface. When the surface is hydrophilic, the drop will spread on the surface giving a large contact area and a low contact angle. When the surface is hydrophobic, on the other hand, the drop will minimize its contact with the surface and the contact angle will be large (van Oss 1994).

Figure 8.3. *Schematic pictures of a drop of liquid on a solid substrate: a) wetting surface (hydrophilic) and b) non-wetting surface (hydrophobic).*

Wetting of a paper is a two-stage process. Wetting is essential if liquid is to be transferred at all, and the first stage relates to this transfer. The wettability of the paper surface is a measure of the paper's affinity for the liquid and in the absence of this affinity no transfer occurs. The second stage involves further wetting of the surface for a certain time before absorption can commence (Bristow 1967).

The contact angles were measured on a FTA 200 Dynamic Contact Angle Analyzer from First Ten Ångstroms (Portsmouth, VA USA) using a drop of de-

_____

ionized water. The contact angles at 0.1 s and 2 s were monitored and the average of at least twelve measurements was calculated (Paper III, Paper IV). Contact angle measurements were performed at 23°C and 50% RH.

8.1.1 Results – contact angles

Contact angles were measured on liner and greaseproof paper sized with starch solutions of different pHs at different application temperature (Paper III), and on pre-coated board and liner sized with starch solutions at 23°C and 50% RH with the addition of different concentrations of glycerol (Paper IV).

In Paper III, the application temperatures were 23°C and 70°C. All substrates were calendared before measuring the contact angles. The contact angles are summarized in *Table 8.1* and *Table 8.2*. The reference starch was used only for sizing the liner and not the greaseproof paper.

Table 8.1. *Contact angles of water (23°C, 50% RH) at 0.1 s for substrates sized with HM starch at 23°C and 70 °C. Contact angle for liner sized with conventional cationic starch (pH 8) was measured to 78 ± 3 at 23°C and 75 ± 2 at 70°C, and for greaseproof paper 70 ± 2°C at 23°C and 68 ± 1°C at 70°C.*

pH	Charge (µeq/g)	Liner 23°C	Greaseproof 23°C	Liner 70°C	Greaseproof 70°C
3.3	82	108 ± 5	69 ± 2	107 ± 4	73 ± 2
5.1	85	108 ± 5	72 ± 4	110 ± 4	74 ± 3
6.3	110	101 ± 5	71 ± 3	109 ± 4	77 ± 3
9.1	118	104 ± 5	N/M	110 ± 4	N/M

Table 8.2. *Contact angles of water (23°C, 50% RH) at 2s for substrates sized with HM starch at 23°C and 70°C. Contact angle for liner sized with conventional cationic starch (pH 8) was measured to 67 ± 3 at 23°C and 63 ± 3 at 70°C, and for greaseproof paper 71 ± 2°C at 23°C and 74 ± 1°C at 70°C.*

pH	Charge (µeq/g)	Liner 23°C	Greaseproof 23°C	Liner 70°C	Greaseproof 70°C
3.3	82	104 ± 5	68 ± 2	105 ± 4	74 ± 2
5.1	85	97 ± 4	72 ± 4	105 ± 5	74 ± 3
6.3	110	93 ± 5	71 ± 3	106 ± 5	76 ± 3
9.1	118	94 ± 4	N/M	107 ± 4	N/M

Sizing with HM starch showed higher contact angles compared to both the reference starch and the unsized liner. For short contact times (0.1s) the pH of the starch solution had no effect at either application temperature. However, as the contact time increased, the contact angels decreased at application at 23°C. This increase indicates an absorption effects on the substrate. Since the contact angles were higher at higher application temperature (70°C) and roughly the same over the time scale of the measurement (0.1-2 s), this indicates that the liner surface had a more hydrophobic character when the application temperature was well above the critical temperature for phase separation.

In Paper IV, pre-coated board and liner were surface-sized with PONP, HONP, HONP$_S$ (supernatant) and HONP$_P$ (precipitate) at 23°C and 50% RH. *Table 8.3* summarizes the contact angles for pre-coated board sized with PONP, HONP, HONP$_S$ and HONP$_P$ with different glycerol contents.

Table 8.3. *Contact angles (23 °C, 50% RH) of water on samples coated at 23 °C with starch solutions*.

Board 255 g/m^2	Glycerol (pph)	Contact angle (°)	
		0.1 s	2.0 s
Uncoated		100.8 ± 2.6	89.4 ± 1.9
PONP	0	51.7 ± 1.0	51.1 ± 1.0
	15	40.7 ± 0.9	40.9 ± 0.8
	30	41.7 ± 1.2	41.6 ± 1.5
HONP	0	61.4 ± 3.6	61.6 ± 3.6
	15	59.1 ± 3.1	59.1 ± 3.4
	30	59.3 ± 2.6	59.0 ± 2.8
HONP$_S$	0	57.8 ± 1.3	58.0 ± 2.0
	15	57.4 ± 1.7	57.0 ± 1.8
	30	56.1 ± 0.7	56.0 ± 0.8
HONP$_P$	0	70.7 ± 2.8	70.8 ± 2.2
	15	71.1 ± 2.5	68.9 ± 2.1
	30	69.5 ± 2.7	69.1 ± 2.5

The contact angle on the pre-coated board decreased upon starch application. PONP without the addition of glycerol gave a higher contact angle than PONP with glycerol. HONP and HONP$_S$ showed no significant difference with or without glycerol. The HONP$_P$ gave the highest contact angles, and thus the hydrophobic character was highest for this material. The HONP$_P$ contained a

_____

higher fraction of hydrophobic modification (analyzed by N-determination) than the HONP$_S$, indicating a hydrophobic contribution from the aliphatic side group. Sizing the liner with PONP (Paper IV) gave lower contact angles compared to unsized liner, whereas HONP showed higher contact angles compared to un-sized liner. The results indicated an improvement in hydrophobic character of the surface when sizing with glycerol-free HONP compared to unsized liner. Addition of glycerol to HONP decreased the contact angles since glycerol promotes water uptake.

Addition of a cationic surfactant, DoTAC, to the HONP starch solution prior to sizing (23°C) liner gave lower contact angles than for starch solution in the absence of surfactant (Paper III). Concentrations of surfactant slightly below CMC gave decreased contact angles at both application temperatures. This indicates that the surfactants migrated to the surface of the paper as the surfactant concentration increased and that the formation of complexes between HM starch and surfactant did not prevent the increased hydrophilic character of the surfaces due to presence of surfactant molecules.

8.1.2 Free films

The contact angle of water on PONP films increased by the addition of glycerol (*Table 8.4*). For HONP on the other hand, the highest contact angle was observed for films without glycerol. This shows that glycerol leads to a decrease in the hydrophobic character of the HONP surface, as was also found with for sized samples (8.1.1).

HONP$_S$ showed roughly the same contact angle for all films, which indicates that glycerol does not affect the surface properties of these film, probably because the solid part of the starch solution was removed. The HONP$_S$ seemed to have a more hydrophobic character than the HONP. The low hydrophobic character of the HONP may be due to inhomogeneities in these films, due to some particulate precipitation upon film formation. The results for the free films were in agreement with those for the sized samples, indicating that HONP starch will probably have a positive effect on the surface characteristics if used in coating formulas.

Table 8.4. *Contact angles (23 °C, 50% RH) of water of free films. Cooked HONP without glycerol and with 15 pph glycerol, and HONP supernatant with 15 pph glycerol did not form coherent films but pieces sufficiently large for contact angle analyses were obtained.*

Free films	Glycerol (pph)	Film thickness (μm)	Contact angle (°)	
			0.1 s	2.0 s
PONP	0	108 ± 3	52.1 ± 5.0	50.1 ± 5.1
	15	116 ± 3	60.2 ± 6.1	58.5 ± 6.6
	30	133 ± 2	61.7 ± 4.5	58.1 ± 3.5
HONP	0	107 ± 4	78.2 ± 5.4	78.0 ± 5.6
	15	120 ± 3	54.4 ± 9.1	51.9 ± 9.1
	30	136 ± 2	39.2 ± 4.0	38.5 ± 3.8
HONP$_S$	0	107 ± 2	87.0 ± 2.9	85.4 ± 3.8
	15	111 ± 1	88.8 ± 7.2	84.4 ± 6.4
	30	120 ± 1	82.4 ± 5.0	79.5 ± 5.4

9   BARRIER PROPERTIES

Starch-based films form excellent barriers to the transport of oxygen (Tomka 1991) and grease (Hullinger 1965), but the water vapor permeability is high due to the hydrophilic nature of starch. Starch-based films are sensitive to humidity and water, and this affects the physical properties of the films during and after film formation (Rindlav-Westling et al. 1998). The same starch films tend to become flexible under humid conditions, and their cohesive and adhesive strengths decrease with increasing water content (Kirby 1986). In general, the barrier properties of polymers are improved by increased crystallinity in the material (Brydson 1995). A high crystallinity should also give films that are less sensitive to the surrounding relative humidity (% RH), i.e. films less sensitive to water.

In order to gain information about the barrier properties of the starches used in this work, the oxygen permeability (OP) was determined for the free films and the water vapor transmission rate (WVTR) was measured on surface-sized substrates and on free films (Paper IV) at different glycerol contents.
The water absorption (Cobb value) was measured to gain information about the water absorption by surface-sized substrates under different conditions (Paper III, Paper IV).

9.1   Oxygen Permeability

Low oxygen permeability (OP) is one of the main requirements for a food packaging material (Paine and Paine 1992). In packaging materials, it is of great importance that the OP is low, since leakage of oxygen can spoil the food due to oxidative reactions of proteins and lipids (Robertson 1993). Increase in crystallinity of synthetic polymers usually means decrease in gas permeability (Rogers 1985).
Oxygen permeability was measured using a Mocon OxTran oxygen permeability tester at 23°C and 50% RH (ASTM D3985-81) (Paper IV). The principle idea is to

apply oxygen on one side of the sample. The oxygen molecules that penetrate the film are transported to a sensor by a stream of nitrogen gas applied on the other side. The voltage created in the sensor is proportional to the oxygen concentration (Forssell et al. 2002).

9.1.1 Results – Oxygen Permeability

The OP of the free films was low and indicates that they provide a good barrier against oxygen (*Table 9.1*). For comparison, OP was measured on commercially available plastic films. The OP-values were for low-density polyethylene film are (LDPE) 1707 ± 28 [$cm^3 \cdot cm/(m^2 \cdot d \cdot bar) \cdot 10^{-2}$] and for polyethylene terephthalate (PET) 12.7 ± 0.5 [$cm^3 \cdot cm/(m^2 \cdot d \cdot bar) \cdot 10^{-2}$]. Since all the films on which we were able to make measurements showed lower OP values, they give a good oxygen barrier compared with the plastic films that are commonly used in the packaging industry today.

Table 9.1. *Oxygen Permeability (23 °C, 50% RH) of free films. Cooked HONP without glycerol, with 15 pph glycerol, and HONP supernatant with 15 pph glycerol did not form coherent films on which OP could be measured.*

Free films	Glycerol (pph)	Film thickness (μm)	OP ($cm^3 \cdot cm/(m^2 \cdot d \cdot bar) \cdot 10^{-2}$)
PONP	0	108 ± 3	3.4 ± 0.3
	15	116 ± 3	5.4 ± 0.2
	30	133 ± 2	7.2 ± 1.9
HONP	30	136 ± 2	7.2 ± 0.0
HONP$_S$	0	107 ± 2	5.6 ± 2.0
	30	120 ± 1	6.6 ± 0.5

It has been shown in the literature (Stading et al. 2001) that oxygen permeability increases with increasing RH and that both amylose and amylopectin films exhibit a higher OP when containing 40% glycerol (due to the increase in water content). Our OP data for PONP and HONP$_S$ agrees well with this. Rindlav-Westling et al. (1998) showed that amylose films exhibits excellent oxygen barrier properties with OP-values of 7 ($cm^3 \cdot cm/(m^2 \cdot d \cdot bar) \cdot 10^{-2}$) while amylopectin films had higher OP.

Besides the crystallinity in the film, the presence of pores and defects strongly affects the permeability properties. An increase in RH that causes plasticization of

_____

amorphous regions can induce swelling of the film and thus increase the pore size and this will have a negative effect on the barrier properties.
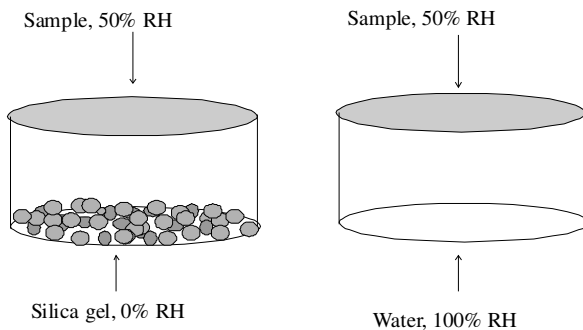

9.2   Water Vapor Transmission Rate

The flow rate of a gas trough paper is inversely proportional to the square root of the molecular weight of the gas (Corte 1958), but for water vapor this flow rate is faster than predicted by its molecular weight.

The rate of mass transfer through a thin plane sheet is characterized by the permeability, P, defined as $P = DS$ where D is the diffusion coefficient and S the solubility. The permeability depends on the molecular weight of the molecules, the concentration or pressure gradient and the thickness of the sheet.

The WVTR of free films (Paper IV) was measured under two different conditions at 23°C and 50% RH (ASTM-E96-90):

i)   With silica gel in the cup.
ii) With de-ionized water in the cup (100 ml)

The first method assumes a moisture gradient of 50%→0% RH and the second 100%→50% RH. *Figure 9.1* shows the cups used: on the left with silica gel at the bottom of the cup, and on the right with water at the bottom of the cup.

Sample, 50% RH   Sample, 50% RH

Silica gel, 0% RH   Water, 100% RH

Figure 9.1. Schematic picture of the gravimetric cups used for determination of water vapor transition rate.

Six replicates of each film were measured. The surface-sized samples were measured under the first conditions only (with silica in the cup). The WVTR was calculated from the linear part of the weight gain curves (*Figure 9.2*), corresponding to a moisture uptake of 4-6%. The water vapor permeability (WVP) was calculated for free films, taking into account the film thickness using

$$P_{WVP} = \frac{P_{WVTR}}{\psi |R_1 - R_2|} \cdot l \qquad\qquad [9.1]$$

where Ψ is the saturation vapor pressure at the test temperature, R_1 is the relative humidity in the test room, R_2 is the relative humidity in the dish, and l is the thickness of the film. For surface-sized samples, WVTR was reported since the sizing thickness was difficult to determine accurately.
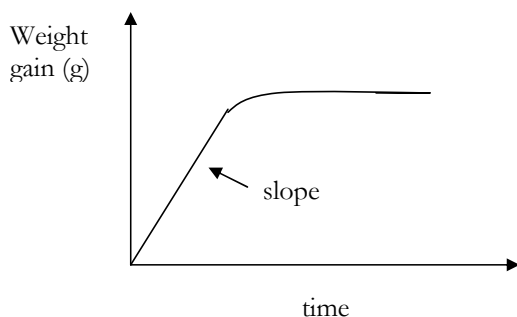
Figure 9.2. *Schematic picture of weight gain as a function of time for determination of WVTR.*

9.2.1 Results – Water Vapor Transmission Rate

The water vapor transmission rate (WVTR) of the free films was measured and the water vapor permeability (WVP) was calculated from the WVTR data, taking into account the film thickness (equation 9.1). As expected (Kimpimäki 1997), the WVTR was found to decrease with increasing film thickness and no change in WVTR was observed for films thicker than ca 100 μm, i.e. the observed effect of glycerol on the WVTR should be solely a chemical effect and not an effect of thickness differences.

PONP films measured with silica gel in the cups showed good water barrier properties and the WVP was further reduced upon addition of glycerol (*Table 9.2*).

Table 9.2. *Water Vapor Permeability of free films (23 °C). Cooked HONP without glycerol and with 15 pph glycerol, and HONP supernatant with 15 pph glycerol did not form coherent films on which the WVP could be determined.*

Free films	Glycerol (pph)	Film thickness (µm)	WVP (g/(Pa·s·m)·10^{-5})	
			50% → 0% RH	100% → 50% RH
PONP	0	108 ± 3	9.8 ± 0.1	29.4 ± 0.3
	15	116 ± 3	4.1 ± 0.1	28.4 ± 0.1
	30	133 ± 2	4.5 ± 0.1	42.1 ± 0.7
HONP	30	136 ± 2	5.9 ± 0.1	43.8 ± 0.5
HONP$_S$	0	107 ± 2	11.8 ± 0.5	29.9 ± 0.8
	30	120 ± 1	7.1 ± 0.5	38.4 ± 0.8

A reduction in WVP was also observed for the HONP$_S$ upon addition of glycerol. Jansson and Järnström (2005) showed that the water vapor permeability was lower for hydroxypropylated starch films plasticized with glycerol than with other plasticizers such as alkyl polyglucoside (APG). Further, they showed that the glass transition temperature (*Tg*) decreased with increasing glycerol content in free films, all in agreement with the theoretical values *Tg* values.

The interaction with a more humid atmosphere, with water in the cups, gave a completely different picture. In all three cases, the WVP was higher at 30 pph glycerol than in the absence of glycerol and was almost identical for all the starch films. This is probably due to the hydroscopic properties of glycerol.

Table 9.3 summarizes the WVTR values for pre-coated board (Performa Natura) sized with PONP, HONP, HONP$_S$ and HONP$_P$. Upon sizing with the different starches, no water vapor barrier was observed. With glycerol-free surface sizes, PONP gave the lowest WVTR. Within the HONP-series, no significant difference between the cooked HONP and HONP$_S$ was observed. On the other hand, when glycerol was added there was a lowering of the WVTR compared to the values for unsized substrate. The HONP$_P$ was dissolved in hot water and applied to the board substrate to investigate its efficiency as a sizing material. The WVTR decreased with addition of glycerol to HONP$_P$. The lower WVTR values for

HONP$_P$ were expected since the precipitate contains a higher amount of hydrophobic tails compared to the supernatant and the original starch solution.

Table 9.3. *Water Vapor Transmission Rate (23 °C) for board sized with different starch solutions. Measurements performed with silica in the cup.*

Performa Natura, 255 g/m^2	Glycerol (pph)	WVTR (g/m^{2}d)
Uncoated		341± 5
PONP	0	295 ± 5
	15	266 ± 3
	30	254 ± 2
HONP	0	318 ± 3
	15	290 ± 4
	30	264 ± 2
HONP$_S$	0	312 ± 6
	15	295 ± 4
	30	280 ± 4
HONP$_P$	0	384 ± 2
	15	250 ± 11
	30	240 ± 5

9.3 Water absorption (Cobb)

The Cobb method is used to determine the water resistance of a sized substrate in contact with liquid water. The surface of the sample is exposed to water for a certain time and the amount of liquid absorbed is determined gravimetrically (Cobb and Lowe 1934). The lower the Cobb value, the less water penetrates into the sample. The hypothesis with the temperature-responsive starches was that if the application temperature of the starch solution was above the critical temperature for phase separation, the Cobb value should be lower than when the starch solution was applied at room temperature, because the starch would form a more uniform film when left to cool on the paper and the phase separation would occur on the paper surface.

The Cobb$_{60}$ value was measured according to ISO 535. Average of six measurements for the liner and three measurements for the greaseproof paper were calculated.

9.3.1 Results – Cobb value

The $Cobb_{60}$ value was measured on liner (with no internal or surface sizing) and greaseproof paper after calendaring (Paper III) and on liner and pre-coated board (Paper IV) without calendaring.

Table 9.4 summarizes the $Cobb_{60}$ values on liner and greaseproof sized with HM starch at different application temperatures and with different solution pHs (Paper III). It was observed that the Cobb value was lower when the application temperature was above the critical phase separation temperature at low pH values. A lower pH gave somewhat lower Cobb value than the higher solution pH when application temperature was 70°C, but there was no great difference at either application temperature or pH, although a slight reduction was observed compared to the cationic reference starch and a larger reduction compared to the unsized liner (185g/m², and almost complete penetration). The greaseproof paper showed a slight increase in Cobb value at low pH, but no essential difference compared with unsized greaseproof paper (26.5 g/m²) because of very little pore sorption in greaseproof paper.

Table 9.4. $Cobb_{60}$ values on liner and greaseproof paper sized with HONP starch solution of 8 wt%. $Cobb_{60}$ values on liner with the reference starch (pH 8) were 140 g/m² and 143 g/m² at 20 °C and 70 °C respectively.

Temperature (°C)	pH	q (µeq/g)	$Cobb_{60}$ (g/m²)	
			Liner	Greaseproof
20	3.27	82	141 ± 3	30.3 ± 2.1
	5.09	85	139 ± 3	24.0 ± 1.9
	6.32	110	145 ± 3	25.9 ± 2.0
70	3.27	82	128 ± 3	25.3 ± 2.1
	5.09	85	139 ± 3	25.6 ± 2.0
	6.32	110	139 ± 3	25.5 ± 2.2

$Cobb_{60}$ values for sized substrates are summarized in *Table 9.5* (Paper IV). The unsized board had a $Cobb_{60}$ value of 27 g/m² which was greatly reduced when sized with PONP and HONP. The $HONP_S$ gave a higher $Cobb_{60}$ value than the HONP, which indicates a loss in hydrophobicity upon removal of the particulate fraction.

Table 9.5. *Cobb$_{60}$ values for liner and board sized with starch of different glycerol content at 23°C and pH 8.*

	Glycerol (pph)	Cobb$_{60}$ (g/m^2)	
		Board, 255 g/m^2	Liner, 140 g/m^2
uncoated		27 ± 2	165 ± 3
PONP	0	18 ± 1	47 ± 1
	15	21 ± 3	45 ± 1
	30	20 ± 1	57 ± 1
HONP	0	18 ± 1	120 ± 3
	15	17 ± 2	50 ± 2
	30	17 ± 1	52 ± 8

Cobb$_{60}$ values for the liner were interesting (Table 9.5, last column). The unsized liner had a very high Cobb value and the substrate was almost totally penetrated by the water after sixty seconds. However, when coated with PONP, the Cobb$_{60}$ values dropped dramatically. With HONP, the reduction in the Cobb$_{60}$ value was observed on samples containing glycerol (both 15 and 30 pph). It was observed in Paper IV that HONP did not form continuous films as PONP, but upon addition of glycerol film formation was possible. This may indicate that the HONP required a plasticizer to facilitate film formation. The film forming properties were of great importance for a low Cobb$_{60}$ value for both PONP and HONP starch. It was not possible to used HONP$_S$ in the surface sizing trials on liner since the paper was completely penetrated during the sizing experiment, probably due to less solid material in the supernatant solution.

10   MECHANICAL PROPERTIES OF FREE FILMS

DMTA is an abbreviation for Dynamic Mechanical Thermal Analysis. DMTA is one of the most versatile thermal analysis methods available and it provides a considerable amount of information about a sample in a single test. This information includes important material property data together with information about the relationship between the materials' chemical composition and its mechanical behavior. Dynamic-mechanical tests are generally more informative than static tests, partially because they make it possible to study very rapid high-frequency-events in the material (Seymour and Carraher 1992). In dynamic tests, heat is generated in the test sample and this reduces its stiffness and strength and therefore leads to premature failure or enhanced creep. DMTA is a technique based on forced vibration and in this work a sinusoidal frequency was applied to the sample.

DMTA is a test method in which the material is characterized in terms of its modulus, elasticity, viscosity, damping behavior and glass transition temperature and how these change with strain, strain rate, temperature or oscillatory frequency. In a DMTA test, an oscillating strain is applied to the sample and the resulting stress developed in the sample is measured (Hedenqvist 2002).

The viscoelastic properties of a polymer change considerably with temperature. Viscoelastic materials experience relaxation transitions associated with molecular mechanisms. These transitions mark a change in mechanical and other properties and the temperature at which these occur is referred to as the glass transition temperature (Tg) for amorphous materials and the melting point (T_m) for crystalline polymers (Seymour and Carraher 1992).

Two different moduli can be derived to describe the viscoelastic properties of a material: an elastic modulus (E') in phase with the strain (solid contribution), and a loss modulus (E'') in phase with the strain rate, 90° out of phase with the strain

(liquid contribution). The phase difference between stress and strain is the damping (δ) which is related to the physical state and the molecular mobility of the polymer. The higher the liquid viscosity, the higher the damping and the larger the phase shift between stress and strain. A positive damping means that the stress is ahead of the strain. The cyclic stress and strain can be derived (Painter and Coleman 1997) as

$$\varepsilon = \varepsilon_0 \sin(\omega t) \qquad\qquad [10.1]$$

$$\sigma = \sigma_0 \sin(\omega t + \delta) \qquad\qquad [10.2]$$

where ε_0 and σ_0 refer to the amplitude, t is the time and ω is the angular frequency. The relationship between the two moduli is well known and expressed by

$$E^* = E' + iE'' \qquad\qquad [10.3]$$

where E^* is the complex modulus. Further, the damping can be expressed as

$$\tan\delta = \frac{E'}{E''} \qquad\qquad [10.4]$$

The mechanical behavior of free films (Paper IV) was analyzed using a dynamic mechanical analysis DMA/SDTA861 from Mettler Toledo (Schwerzenbach, Switzerland) in the tensile mode. This instrument uses the forced vibration-technique, which means the stress response is measurement upon applying sinusoidal strain and the frequency dependence can be obtained. Dynamic oscillating frequency sweeps were performed at 50% RH at constant temperature (23°C).

10.1 Results - DMTA

The mechanical properties of free starch films were analyzed by oscillating humidity scans (Paper IV). The storage modulus (at 10Hz) from the oscillatory

tests (average of six measurements) at 50% RH and 23°C for films of PONP, HONP and HONP$_S$ are summarized in *Figure 10.1*.
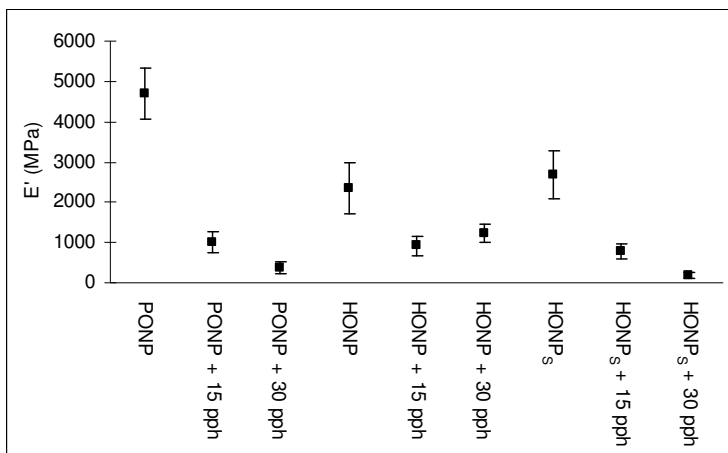

Figure 10.1. *Storage modulus for PONP, HONP and HONP$_S$ films with different glycerol content at 10 Hz, 23°C and 50% RH. Average of six measurements were calculated and indicated with error bars.*

The storage modulus decreased upon addition of glycerol for all films. Glycerol allows the films to take up more water, and both glycerol and water have plasticizing effects on the starch and make them less stiff and more flexible.

Stading et al. (2001) showed that the storage modulus for glycerol-plasticized films of amylose and amylopectin (prepared at 50% RH) decreased upon addition of glycerol in agreement with the present work. Myllärinen et al. (2002b) showed that films of amylopectin were more brittle than films of amylose.

If the surrounding RH was to be increased, the storage modulus should decrease (Stading et al. 2001; Myllärinen et al 2002b; Lourdin et al. 1997) due to the plasticizing effect of water on the starch films. The glycerol also promotes water uptake of the films, which should make films with high content of glycerol and at high surrounding RH very flexible with low storage modulus. The plasticization should lead to a more flexible network and allow possibilities for rearrangements in the network structure. This was not studied in this work.

With increasing amount of glycerol in the films, the film thickness increased for all films. The storage modulus as a function of film thickness was measured on PONP films (*Figure 10.2*). It was concluded that the measurements showed quite large deviations, with the thickest film showing the largest variance. However, the films investigated by DMTA all had thicknesses between 103 to 136 µm depending on glycerol content and according to Figure 10.2, they all fall within the same values in terms of storage modulus in this thickness interval. It can be concluded from Figure 10.2 that the PONP films had a higher storage modulus than the commercially available plastic films used in the packaging industry today.
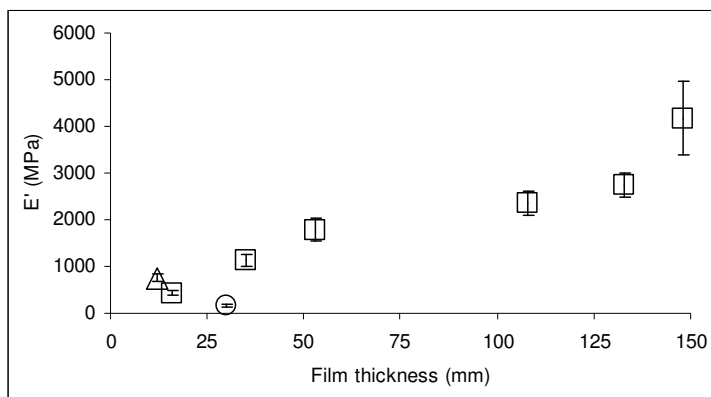
Figure 10.2. *The storage modulus as a function film thickness of PONP measured at 10 Hz, 23°C and 50% RH where: □ PONP, Δ PET, and ○ LDPE.*

11   CONCLUSIONS

Aqueous solutions of HM starches precipitated as a compact solid or formed a network gel upon cooling. The process was governed by the polymer charge. When the net charge of the polymer was almost zero, less precipitation was observed indicating that the net polymer charge governed the balance between precipitation and gel formation. In the presence of surfactant, a stabilizing effect was observed and phase separation was prevented.

When oxidized amylose was mixed with HM amylopectin, an inclusion complex was formed. A model for the destabilizing mechanism (the phase separation) of the hydrophobically modified starches was proposed as well as a model that explains the difference in stabilizing capacity between the investigated cationic and anionic surfactants. The net charge density of the starch and the charge of the surfactant determined whether or not an inclusion complex would form between them. Important mechanisms for the stability of the starch seemed to be formation of mixed micellar-like structures between the hydrophobic chain of the starch and the surfactant along the starch backbone in addition to formation of inclusion complexes between the starch and the surfactant.

The HM starches show promising features for applications in the paper industry. The final surface properties of paper surface-sized with HM starch are dependent of the application temperature, the surfactant concentration and the charge of the polymer. The temperature-responsive properties of these HM starches can be used to achieve improved water resistance on liner in terms of $Cobb_{60}$ values and the film forming properties were of great importance to achieve low Cobb values. The contact angles indicated that the hydrophobic character of the surface was enhanced when application temperature was above the phase separation temperature. By adjusting the pH of the starch solution to a high pH and performing surface sizing above the critical phase separation temperature, enhancements in hydrophobic character of the surface-sized liner were obtained.

Upon addition of surfactant, there was a substantial deterioration in hydrophobic character due to the surfactant migration to the surface.

The starch films showed good oxygen barrier, while the water vapor barrier was poor. Addition of glycerol gave reduced water vapor transmission, but still no barrier effect. The storage modulus of the starch films decreased upon addition of glycerol due to plasticizing effects and the glycerol made them more flexible and less stiff. The glass transition temperature decreased upon addition of glycerol. The water sorption was reduced in terms of $Cobb_{60}$ when sized with starch solutions containing glycerol.

ACKNOWLEDGEMENTS

REFERENCES

Banks, W.; Greenwood, C. T.: *Starch and its components*. University Press, Edinburgh, **1975**.

Barnes, H. A., Hutton, J. F., Walters, K.: *An Introduction to Rheology*. Elsevier Science B.V., Amsterdam, Netherlands, **1989.**

Biliaderis, C. G., and Galloway, G.: Crystallization behavior of amylose-V complexes: structure-property relationship. *Carbohydr. Res.*, **1989**, *189*, 31-48.

Bizot, H., LeBail, B., Leroux, J., Davy, P., Parker, P., Buléon, A.: Calorimetric evaluation of the glass transition in hydrated, linear and branched polyanhydroglucose compound. *Carbohydr. Polym.*, **1997**, *32*, 33-50.

Bristow, A.: Liquid absorption into paper during short time intervals. *Svensk Papperstidning*, **1967**, *19*, 623-629.

Brydson, J. A.: *Plastic materials*. Butterworth-Heinemann Ltd., Oxford, **1995**.

Buléon, A.; Colonna, P.; Planchot, V.; Ball, S.: Starch granules: structure and biosynthesis. *Biol. Macromol.*, **1998**, *23*, 85-112.

Buléon, A., Tran, V.: Systematic conformational search for the branching point of amylopectin. *Int. J. Biol. Macromol.*, **1990**, *12*, 345-352.

Champeney, D.C., Kaddour, O. F.: Ionic mobility and dielectric relaxation in supercooled liquid KCl-glycerol solutions. *Molecular Physics*, **1984**, *52*, 509-523.

Chien, J.T., Lien, Y.Y., Shoemaker, C.E.: Effect of polarity of complexing agents on thermal and rheological properties of rice starch gels. *Cereal Chem.*, **1999**, *76*, 837-842.

Cobb, R. M., Lowe, D. V.: A sizing test and a sizing theory. *Tech. Assoc. Pap.*, **1934**, *17*, 213-216.

Corte, H.: *The porous structure of paper*, In Fundamentals in Papermaking Fibres, Transactions of the Symposium 1957, British Paper and Board Makers' Association, **1958**, pp. 301-331.

Cram, D. J.: The design of molecular hosts, guests, and their complexes. *Science*, **1988**, *240,* 760-767.

Cushing, M. L.; Schuman, K. R.: Fiber attraction and interfiber bonding-the role of polysaccharide additives. *Tappi Journal*, **1959**, *42*, 1006-1016.

Eliasson, A.-C.: Interactions between starch and lipids studied by DSC. *Thermochim. Acta*, **1994**, *246*, 343-356.

Eliasson, A.-C., Kim, H.-R.: A dynamic rheological method to study the interaction between starch and lipids. *J. Rheol.*, **1995**, *39*, 1519-1534.

Evans, D. F., Wennerström, H.: *The Colloidal domain, Where Physics, Chemistry, Biology and technology meet.* 2nd ed., Wiley, New York, **1999**.

Fellers, C., Norman, B.: *Pappersteknik.* Kungliga tekniska Högskolan, Stockholm, **1996**.

Fleer, G. J., Cohen Stuart, M. A., Scheutjens, J. M. H. M., Cosgrove, T., Vincent, B.: *Polymers at Interfaces.* Chapman & Hall, University Press, Cambridge, **1993**.

Flory, P. J. J.: Thermodynamics of high polymer solutions. *Chem. Phys.*, **1942**, *10*, 51-61.

Flory, P. J.: *Principals of Polymer Chemistry.* Cornell University Press, Ithaca, New York, **1953**.

Forssell, P., Lahtinen, R., Lahelin, M., Myllärinen, P.: Oxygen permeability of amylose and amylopectin films. *Carbohydr. Polym.*, **2002**, *47*, 25-129.

French, J. D.: Fine structure of starch and its relationship to the organization of starch granules. *J. Jpn. Soc. Starch Sci. (Denpun Kagaku)* **1972**, *19*, 8-25.

Gallant, D. J., Bouchet, B., Baldwin, P. M.: Microscopy of starch: evidence of a new level of granule organization. *Carbohydr. Polym.*, **1997**, *32*, 177-191.

Gidley, M. J.: Quantification of the structural features of starch polysaccharides by n.m.r. spectroscopy. *Carbohydr. Res.*, **1985**, *139*, 85-93.

Glass, J.E.: *Polymers in Aqueous Media.* Glass, J. E (Ed.), American Chemical Society, Washington DC, vol. 223, **1989**.

Glittenberg, D., Becker, A.: Cationic starches for surface sizing. *Paper technology*, **1998**, *39*, 37-41.

Gmelin, E. Classical temperature-modulated calorimetry: A review. *Thermochim. Acta*, **1997**, *304/305*, 1-26.

Godet, M. C., Buléon, A., Tran, V., Colonna, P.: Structural features of fatty acid-amylose complexes. *Carbohydr. Polym.*, **1993a**, *21*, 91-95.

Godet, M. C., Tran, V., Delage, M. M., Buléon, A.: Molecular modeling of the specific interactions involved in the amylose complexation by fatty acids. *Int. J. Biol. Macromol.*, **1993b**, *15*, 11-16.

Godet, M. C., Bizot, H., Buléon, A.: Crystallization of amylose - fatty acid complexes prepared with different amylose chain lengths. *Carbohydr. Polym.,* **1995**, *27*, 47-52.

Gracza, R. *Minor constituents of starch (chap. 6),In Starch: Chemistry and Technology*, Vol. 1, Whistler, R. L. and Paschall, E. F. (Eds)., Academic Press, New York, **1984**.

Gregory, J.: Turbidity fluctuations in flowing suspensions. *J. Colloid Interface Sci.*, **1985**, *105*, 357-371.

Gruber, J. V., Konish, P. N.: Aqueous viscosity enhancement through helical inclusion complex cross-linking of a hydrophobically-modified, water-soluble, cationic cellulose ether by amylose. *Macromolecules*, **1997**, *30*, 5361-5366.

Hedenqvist, M.: *Mechanical properties of polymers; viscoelastic properties.* Course compendium, Royal Institute of Technology, Stockholm, **2002**.

Helbert, W., Chanzy, H.: Single crystals of V-amylose complexed with n-butanol or n-pentanol: structural features and properties. *Int. J. Biol. Macromol.*, **1994**, *16*, 207-213.

Hester, R. D. and Squire, D. R., Jr.: Rheology of Waterborne Coatings. *J. Coatings Techn.*, **1997**, *69*, 109-114.

Hizakur, S.: Polymodal distribution of the chain lengths of amylopectins, and its significance. *Carbohydr. Res.,* **1986**, *147*, 342-347.

Huggins, M. L.: Some Properties of Solutions of Long-chain Compounds. *J. Phys. Chem.*, **1942**, *46*, 151-158.

Hullinger, C. H.: Starch film and coating. *Cereal Sci. Today*, **1965**, *10*, 508-510.

Imberty, A., Buléon, A., Tran, V., Perez, S.: Recent advances in knowledge of starch structure. *Starch*, **1991**, *43*, 375-384.

Imberty, A., Chanzy, H., Perez, S., Buléon, A., Tran, V.: The double-helical nature of the crystalline part of A-starch**.** *J. Mol. Biol.*, **1988**, *201*, 365-378.

Imberty, A., Perez, S.: Crystal structure and conformational features of α-panose. *Carbohydr. Res.,* **1988**, *181*, 41-55.

Immel, S., Lichtenthaler, F. W.: The hydrophobic topographies of amylose and its blue iodine complex. *Starch*, **2000**, *52*, 1-8.

Jansson, A., Järnström, L.: Barrier and mechanical properties of modified starches. *Cellulose*, **2005**, *12*, 423-433.

Jenkins, P. J., Donald, A. M.: The influence of amylose on starch granule structure. *Int. J. Biol. Macromol.*, **1995**, *17*, 315-352.

Järnström, L., Hansson, P., Nilsson, P.-O., Brossmer, C. and Wiklander, K.: Hydrophobically modified cationic starches for surface treatment. *TAPPI Coating Conference and Trade Fair*, May 1-4, **2000**, Washington, DC.

Jönsson, B., Lindman, B., Holmberg, K., Kronberg, B.: *Surfactants and polymers in solution*. Wiley, New York, **1999**.

Kan, C. S.: Role of particle size in latex deformation during film formation. *J. of Coatings Techn.*, **1999**, *71*, 89-97.

Karkalas, J., Raphaelides, S.: Quantitative aspects of amylose-lipid interactions. *Carbohydr. Res.*, **1986**, *157*, 215-234.

Kearney, R. L., Maurer, H. W. (Ed): *Starch and Starch Products in Paper Coating*. Tappi Press, Atlanta, USA, **1990**.

Kimpimäki, T. and Savolainen, A.: Barrier dispersion coating of paper and board, in Brander, J. and Thorn, I. *Surface Application of Paper Chemicals*, Blackie Academic & Professional, **1997**, pp. 208-228.

Kirby, K. W.: *Textile industry*. In: Wurzburg O.B. (ed.) *Modified starches: Properties and uses*. CRC Press Inc., Boca Raton, Florida, **1986**, pp. 229-251.

Koch, H., Brommer, H.D., and Koppers, J.: Analytical investigations on phosphate cross-linked starches. *Die Stärke*, **1982**, *34*, 16-21.

Kubik, S., Holler, O., Steinert, A., Tolksdorf, M., Wulff, G.: Inclusion compounds of derivatized amyloses. *Macromol. Symp.,* **1995**, *99*, 93-102.

Larson, R. G.: *The Structure ad Rheology of Complex Fluids*. Oxford University Press, New York, **1999**.

Landoll, L. M.: Nonionic Polymer Surfactant. *J. Polym. Sci.: Polym. Chem. Ed.*, **1982**, *20*, 443-455.

Lee, H. L.; Shin, J. Y.; Hoh, C.-H.; Ryo, H.; Lee, D.-J.; Sohn, C. Surface sizing with cationic starch: its effect on paper quality and papermaking process. *Tappi Journal*, **2002**, *1*, 34-40.

Lehtinen, E. (Ed): *Pigment Coating and Surface Sizing of Paper*. Fapet Oy, Helsinki Finland, **2000**.

Lindman, B., Carlsson, A., Gerdes, S., Karlström, G., Piculell, L., Thalberg, K. and Zhang, K.: "Polysaccharide-Surfactant Systems: Interactions, Phase Diagrams and Novel Gels" in "Food Colloids and Polymers: Stability and Mechanical Properties". P. Walstra and E. Dickinson (Eds.), RSC, **1993**, pp. 113-125.

Lindman, B., Wennerström, H.: Amphiphile aggregation in aqueous solution. *Top.: Curr. Chem.,* **1980**, 87, 1-83.

Lourdin, D., Bizot, H. and Colonna, P.: "Antiplasticization" in Starch-Glycerol Films?. *Appl. Polym. Sci.,* **1997**, *63*, 1047-1053.

Maurer, H. W (Ed): *Starch and Starch products in surface sizing and paper coating.* Tappi Press, Atlanta, **2001**.

McIntyre, D. D., Ho, C., Vogel, H. J.: One-dimensional nuclear magnetic resonance studies of starch and starch products. *Starch*, **1990**, *42*, 260-267.

Mikus, F. F., Hixon, R. M., Rundle, R. E.: The complex of fatty acids with amylose. *J. Am. Chem. Soc.*, **1946**, *68*, 1115-1123.

Moeller, H. W.: Cationic starch as a wet-end strength additive. *Tappi Journal*, **1966**, *49*, 211-214.

Morrison, W. R., Laignelet, B.: An Improved colorimetric procedure for determining apparent and total amylose in cereal and other starches. *J. Cereal Chem.*, **1983**, *1*, 9-20.

Muhrbeck, P., Tellier, C.: Determination of the phosphorylation of starch from native potato varieties by ^{31}P NMR. *Starch*, **1991**, *43*, 25-27.

Mukarjee, P., Mysels, J. J.: *Critical Micelle concentrations of Aqueous Surfactant Systems.* National Bureau of Standards, Washington DC, **1971**.

Muller, P., Gruber, E., Brossmer, C. and Bischoff, D.: Teilhydrophobierte kationische Stärken fur den Einsatz bei der Oberflächenleimung von Papier. *Int. Papwirtsch.*, **2000**, *2*, T22-T28.

Myllärinen, P., Partanen, R., Seppälä, J., Forssell, P.: Effect of glycerol on behaviour of amylose and amylopectin films. *Carbohydr. Polym.*, **2002a**, *50*, 355-361.

Myllärinen, P., Buléon, A., Lahtinen, R., Forssell, P.: The crystallinity of amylose and amylopectin films. *Carbohydr. Polym.*, **2002b**, *48*, 41-48.

Neimo, L (Ed): *Papermaking Chemistry.* Fapet Oy, Helsinki Finland, **2000**.

Nilsson, G. S., Bergquist, K.-E., Nilsson, U., Gorton, L. Determination of the Degree of branching in normal and amylopectin type potato starch with 1H-NMR spectroscopy: Improved resolution and two-dimensional spectroscopy. *Starch*, **1996**, *48*, 352-357.

Nimz, O., Gessler, K., Usón, I., Sheldrick, G. M., Saenger, W.: Inclusion complexes of V-amylose with undecanoic acid and dodecanol at atomic resolution: X-ray structures with cycloamylose containing 26 ᴅ-glucoses (cyclohexaicosaose) as host**.** *Carbohydr. Res.*, **2004**, *339*, 1427-1437.

Orford, P.D., Parker, R., Ring, S. G., Smith, A. C.: Effect of water as a diluent on the glass transition behaviour of malto-oligosaccharides, amylose and amylopectin. *Int. J. Biol. Macromol.*, **1989**, *11*, 91-96.

Paine, F.A., Paine, H. Y.: *A handbook of food packaging.* Blackie Academic & Professional, Glasgow, **1992**.

Painter, P., Coleman, M.: *Fundamentals of polymer science – An introductory text.* 2nd ed. Technomic Publishing Company, Inc., Lancaster, Pennsylvania, USA, **1997**.

Parker, R., Ring, S. G.: Aspects of the Physical Chemistry of Starch. *J. Cereal Chem.*, **2001**, *34*, 1-17.

Piculell, L., Thuresson, K., Lindman, B.: Mixed solutions of surfactant and hydrophobically modified polymer. *Polym. Adv. Techn.*, **2001**, *12*, 44-69.

Polaczek, E., Starzyk, F., Malenki, K., Tomasik, P.: Inclusion complexes of starch with hydrocarbons. *Carbohydr. Polym.*, **2000**, *43*, 291-297.

Rindlav Å., Hulleman, S. H. D., Gatenholm, P.: Formation of starch films with varying crystallinity. *Carbohydr. Polym.*, **1997**, *34*, 25-30.

Rindlav-Westling, Å., Stading, M., Hermansson, A-M., Gatenholm, P.: Structure, mechanical and barrier properties of amylose and amylopectin films. *Carbohydr. Polym.*, **1998**, *36*, 217-224.

Robertson, G. L.: *Food packaging principles and practice.* Marcel Dekker Inc., New York, **1993**.

Robin, J., Mercier, C., Charbonnier, R., Guilbot, A.: Lintnerized Starches. Gel Filtration and Enzymatic Studies of Insoluble Residues from Prolonged Acid Treatment of Potato Starch. *Cereal Chem.*, **1974**, *51*, 389-405.

Rogers, C. E.: Permeability of gases and vapours in polymers. In *Polymer Permeability*, J. Camyn (Ed), Elsevier, London, UK, **1985**, pp. 11-71.

Rundle, R. E., Edwards F. C.: The Configuration of Starch and the Starch-Iodine Complex. IV. An X-ray Diffraction Investigation of Butanol-Precipitated Amylose. *J. Am. Chem. Soc.* **1943**, *65*, 2200-2203.

Seymour, R. B., Carraher, C. E, Jr.: *Polymer Chemistry An Introduction*. Lakowski, J. J. (Ed), Marcel Dekker, Inc., New York, **1992**.

Skoog, D. A., Leary, J. J.: *Principles of Instrumental Analysis*. Fourth ed., Harcourt Brace & Company, Orlando, Florida, USA, **1992.**

Stading, M., Rindlav-Westling, Å., Gatenholm, P.: Humidity-induced structural transitions in amylose and amylopectin films. *Carbohydr. Polym.*, **2001**, *45*, 209-217.

Stevens, M. P.: *Polymer Chemistry*. Oxford University Press, New York, **1999**.

Svegmark, K.; Hermansson, A-K.: Shear induced changes in the viscoelastic behavior of heat-treated potato starch dispersions. *Carbohydr. Polym.*, **1990**, *13*, 29-45.

Svegmark, K., Helmersson, K., Nilsson, G., Nilsson, P.-O., Andersson, R., Svensson, E.: Comparison of potato amylopectin starches and potato starches – influence of year and variety. *Carbohydr. Polym.*, **2002**, *47*, 331-340.

Swinkels, J.J.M.: Composition and properties of commercial native starches. *Starch*, **1985**, *37*, 1-5.

Tanaka, R., Meadows, J., Phillips, G. O., Williams, P. A.: Viscometric and spectroscopic studies on the solution behavior of hydrophobically modified cellulosic polymers. *Carbohydr. Polym.*, **1990**, *12*, 443-459.

Thuresson, K., Nystroem, B., Wang, G., Lindman, B.: Effect of surfactants on structural and thermodynamic properties of aqueous solutions of hydrophobically modified ethyl(hydroxyethyl)cellulose. *Langmuir*, **1995**, *11*, 3730-3736.

Tomka, I.: *Thermoplastic starch*. In H. Levine & L. Slade, *Water relationships in food*. Plenum Press, New York; **1991**, 66, pp. 627-637.

Turi, E. A. (Ed): *Thermal Characterization of Polymeric Materials*. 2nd ed., Academic Press, Inc., San Diego, **1997**.

Van Os, N. M., Haak, J. R., Rupert, L. A.M.: *Physico-Chemical Properties of selected anionic, cationic, and nonionic surfactants*. Elsevier Science, Amsterdam, **1993.**

Van Oss, C. J.: *Interfacial forces in aqueous media*. Marcel Dekker Inc., New York, **1994.**

Velikov, V., Borick, S., Angell, C.A.: The glass transition of water, based on hyperquenching experiments. *Science*, **2001**, *294*, 2335-2338.

Wesslén, B.: "Amphiphilic Graft Copolymers - Preparation and Properties". *Macromol. Symp.*, **1998**, *130*, 403-410.

Weyer, S., Hensel, A., Schick, C.: Phase angle correction for TMDSC in the glass-transition region. *Thermochim. Acta*, **1997**, *304/305*, 267-275.

Whistler, R. L., BeMiller, J., Paschall, E. F.: *Starch: Chemistry and Technology.* Academic Press, Inc., New York, **1984**.

Williams, D. H., Fleming, I.: *Spectroscopic methods in organic chemistry.* Fifth edition, McGraw-Hill International Limited, Berkshire, England, **1995**.

Winnik, M. A., Yekta, A.: Associative polymers in aqueous solution. *Curr. Opin. in Colloid Interface Sci.*, **1997**, *2*, 424-436.

Wurzburg, O. B. *Modified starches: Properties and uses.* (Ed. O. B. Wurzburg) CRC Press, Boca Raton, Fl., **1986**.

Yamamoto, M., Sano, T., Yasunaga, T.: Interaction of Amylose with Iodine. I. Characterization of Cooperative Binding Isotherms for Amyloses. *Bull. Chem. Soc. Jpn.*, **1982**, *55*, 1886-1889.

Young, A. H. Fractionation of starch. In *Starch: Chemistry and Technology.* R. L. Whistler, BeMiller, J.N., Paschall, E.F. (Eds), Academic Press, Inc., New York, **1984.**

Zobel, H. F.: Molecules to granules: A comprehensive starch review. *Starch,* **1988**, *40*, 44-50.

Properties of modified starches and their use in the surface treatment of paper

The papermaking industry uses a large amount of starch, chemicals and energy. It is important to be able to reduce the amount of chemicals used in the papermaking and surface treatment process, to reduce costs and to make the process even more efficient. Interest in new high-performance starches is great. By using these new types of starches, improved recycling of barrier products may be obtained as well as a reduction in the use of synthetic sizing agents. The objectives of this work were to understand the behavior of temperature-responsive hydrophobically modified starches, where the solubility in water simply can be adjusted by temperature or by polymer charge, to improve the barrier properties, like the water vapor permeability, mechanical properties and water resistance (Cobb and contact angle) of papers surface sized by starch-containing solutions, and to investigate the potential for industrial use of these temperature-responsive starches. It was demonstrated that the temperature-responsive starches phase separate upon cooling and, depending on the charge density of the starch, a particulate precipitation or a gel-like structure was obtained. The starches showed inclusion complexes with surfactant, giving stabilizing effects to the starch. Free films of the temperature-responsive starches showed good oxygen barrier but no water vapor barrier and the mechanical properties decreased upon addition of glycerol.